

AD619526

AF-EOAR 63-76

**ROUGH COMBUSTION  
IN LIQUID ROCKET MOTORS**

**P. D. McCORMACK, S. BIRCH, L. CRANE**

**DUBLIN UNIVERSITY.**

---

---

AF EOAR 63-76

January 1965

Technical Report  
"Rough Combustion in Liquid Fuel  
Rocket Motors"

P.D. McCORMACK, S. BIRCH & L. CRANE.

Engineering School  
Trinity College,  
Dublin,  
Ireland.

The research reported in this document has been sponsored by the  
Office of Scientific Research, OAR  
through the European Office, Aerospace Research, United States  
Air Force.

Contents:

Page 1 to 3	ABSTRACT & LIST OF PAPERS.
Page 4 to 12	PART 1 - " A DRIVING MECHANISM FOR HIGH FREQUENCY COMBUSTION INSTABILITY IN LIQUID FUEL ROCKET ENGINES".
Page 13 to 38	PART 11 - "AN EXPERIMENTAL AND THEORETICAL ANALYSIS OF CYLINDRICAL LIQUID JETS SUBJECTED TO VIBRATION".
Page 39 to 51	PART 111- "PROPERTIES OF TAYLOR VORTICES OF LARGE AMPLITUDE".
Page 52	PART IV - "FUTURE WORK".

## ABSTRACT

The research performed under Grant AF-EOAR-63-76, is reported in three main parts.

### Part 1

This mainly covers the material in the original proposal. A rough model of the rocket combustion process demonstrates that if a modulated flow of fuel could be produced at the injector plate, a repetitive and corresponding variation of combustion pressure would result, and form a driving mechanism for high frequency combustion instability. It must be noted that at the frequencies involved, the inertia of the fuel feed lines would hinder the total fluid column behind the injectors from following. Thus the fuel flow modulation must come from a modulation of the discharge velocity from each orifice, for example, by a change in the pressure at the plane of the orifice exit (this pressure determines the discharge velocity for a given fuel and orifice).

The high 'g' vibrations to which rocket engines are subjected both on the test stand and in flight, suggested that transverse mechanical vibration of the injector plate could induce this fuel flow modulation.

### Part 2

Initial work on the effect of low 'g' vibration on injector behaviour was reported at the 16th AFOSR Meeting on Nantucket Island and in the June 1964 edition of the British Institute of Applied Physics.

It has been established that vibration induces velocity modulation in the jet emerging from the injector. At low 'g' the minute modulation merely serves to trigger the capillary type instability. At high 'g' (greater than 100), the velocity modulation is sufficient to result in a predominant bunching effect in the liquid jet. Spectacular disc formation on the jet is the result. Discs on jets from neighbouring holes can be in phase or out of phase depending on their alignment with respect to the line of vibration.

'Bunching' occurs whether the jet is laminar or turbulent, low velocity or high velocity.

Rayleigh's original analysis has been modified

(a) to specifically incorporate velocity modulation as a trigger mechanism, and to cover second order effects.

(b) to include the 'bunching' effect at least in the transition region where it has not become completely dominant over the capillary effect.

then to couple with an acoustic mode of the chamber to become self sustaining.

A tangential mode of vibration, by including space-wise phase shift in the jet modulation across the injector plate, can initiate the tangential mode of instability. Thus, modes of combustion instability can be related directly to modes of vibration.

### Part 3

The effect of the tangential mode of instability on the boundary layer heat transfer coefficient is considered.

The wall vibrations set up, cause driven vortices of the Taylor-Goertler type with axes parallel to the cylindrical chamber axis.

The increase in the heat transfer coefficient with respect to that in the normal laminar layer, is derived. A small effect was found.

The presence, however, of rotational motion of the chamber gas, associated with the tangential mode, leads to an unsteady vortex motion in the boundary layer, which builds up rapidly. These vortices resemble those observed to be formed between two concentric rotating cylinders.

This vortex growth causes a very significant increase in the heat transfer coefficient which occurs in a very small time (less than  $10^{-2}$  sec). Upper and lower limits of the effect are established.

The increase in heat transfer coefficient, combined with the increase in rate of heat release associated with the tangential mode in a plane close to the injectors, will normally cause rapid chamber wall burn-out.

It is considered that turbulence in the rocket engine boundary layer is unlikely, and that separation is not present. That is to say, a well-ordered and effectively laminar layer exists, even though vortex formation has occurred.

Vorticity induced in the boundary layer due to shear flow in the fluid external to it, is known to have a small effect on the heat transfer coefficient (certainly much less than that due to full vortex formation the boundary layer).

Hence, the only source of appreciable increase in the coefficient is that due to the rapid build-up of the Taylor-Goertler vortex formation with free stream rotational motion.

The work points to a possible way of preventing

## Papers and Reports

### Papers

- (1) "The Effect of Mechanical Vibration on the Break-up of a Cylindrical Water Jet in Air", British Journal of Applied Physics Vol.15, p.743-751 (1964), by P.D. McCormack, S. Birch and L. Crane.
  - (2) "A Driving Mechanism for High Frequency Combustion Instability Liquid Fuel Rocket Engines", Journal of the Royal Aeronautical Society, Vol.60 No. 645 p.633-637 (1964) P.D. McCormack.
  - (3) "An Experimental and Theoretical Analysis of Cylindrical Liquid Jets subjected to Vibration", British Journal of Applied Physics (in the press) P.D. McCormack, S. Birch, L.Crane.
  - (4) "Property of Taylor Vortices of Large Amplitude"
  - (5) "The Tangential Mode of Rocket Engine Burn-Out"
- (Both of these papers are being submitted to the Royal Aeronautical Society.

### Reports

- (1) Admin. Report No.3 AF-EOAR 63-76 July (1964)

### Theses

- (1) "Automation of Multi-element Chemical Equilibria Computations on a Digital Computer" by Dr.P.D. McCormack.

Dissertation in part fulfilment of requirements for an M.Sc. in computer technology from Trinity College, Dublin. (degree awarded 1964).

- (2) "The Effect of Vibration on the Break-up of Liquid Jets" by S. Birch. Submitted to Trinity College, Dublin, for the degree of M.Sc. (awarded October, 1964).

### Talks and Papers Presented

- (a) 17th AFOSR Contractor's Meeting on Liquid Propellant Rocket and Air-breathing Combustion Research, July, 1964, at Pasadena, California. "Theoretical and Experimental Analysis of the Behaviour of Liquid Jets subjected to High "g" Mechanical Vibrations".
- (b) Three lectures on the work done so far on AF-EOAR 63-76 to the faculty members, graduate and undergraduate students, at the Thayer School of Engineering, Dartmouth College, New Hampshire, November 3rd-7th, 1964.

PART 1

**TITLE:** "A driving Mechanism for High  
Frequency Combustion Instability  
in Liquid Fuel Rocket Engines".

## Section 1. Introduction

The problem of combustion pressure oscillation in liquid-fuel rocket motor operation has long been the subject of theoretical and experimental investigations.

The low frequency (less than 200 c.p.s.) type of oscillation, known as "chugging", has been thoroughly analysed and the problem solved - see Crocco, 5th Combustion Symposium, p.164.

This paper is concerned with the more complex (and more destructive) high frequency oscillations, covering a range from about 1,000 to 6,000 c.p.s. Such oscillations can resonate with the acoustical modes of the combustion chamber. Longitudinal, tangential and radial oscillating modes have been observed.

Pickford and Peoples (1) have put forward a very comprehensive treatment of the inherent stability of the combustion process. However their work involves the postulation of a basic pressure perturbation which is not defined. This results in the use of a rather incomplete perturbation index.

Fuel injection is an important factor in high intensity combustion systems, whereby the atomization process is used to create the maximum practical surface area of liquid fuel to aid rapid evaporation, has been recognised for many years.

Under conditions of high temperature and pressure, chemical kinetics heretofore was considered as not being a contributing factor. Characteristic reaction times are of the order of  $10^{-7}$  sec, in comparison with characteristic chamber frequencies with periods in the region of  $10^{-3}$  sec. Most of the residence time in the combustion chamber is spent in the physical processes of liquid atomization, drop evaporation and gas phase mixing, prior to reaction. All of these factors are closely related to the injector design.

Several theories of combustion system performance have been postulated on the basis of evaporation as the only rate controlling process. <sup>(2,3)</sup> However, practical studies indicate differences between the predicted system behaviour and that actually observed. In any case, it does not appear that the evaporation process alone can explain the role of the injector as an initiating instability mechanism.

Progress in theory and experiment then, so far has only led to certain rough rules which act as guides in the design stage of rocket engines. Pressure oscillations can, and still do, occur at random in even the most conservatively designed units, leading at least to severe impairment of operation.

The establishment of the basic cause of this phenomenon

The presence of random combustion pressure fluctuations in a smoothly running engine is easily demonstrated. The amplitudes are seldom greater than about one or two percent of the steady pressure. These fluctuations could be a consequence of discontinuous energy injection into the system. Any mechanism which would synchronize events at all injectors, could then cause considerable pressure oscillations.

It is known that both on the test stand<sup>(4)</sup> and in actual flight,<sup>(5)</sup> the rocket engine can be subjected to high 'g' high frequency vibration (See Appendix 1).

In the 140,000 lbs thrust Atlas type booster, taken later as an example, theory<sup>(6)</sup> predicts a 30 'g', 1000 c.p.s. response to the component of the engine noise field arriving at the vehicle surface. On test stands much higher 'g' values have been observed.

It is contended that this vibration will cause periodic (at the applied frequency) variation of the fuel flow rate from an injector. This "bunching" of fluid moreover, will be synchronized at each injector (all the holes will be synchronized provided the injector plate is vibrating in the n - 1 mode). Experimental verification and investigation of this phenomena has occupied most of the work during this grant and will be reported in Part 2.

Thus, with synchronization, the fuel flow rate entering the combustion zone will be modulated at the vibration frequency.

It is well known that under proper conditions of phasing between mass rate and chamber pressure, spontaneous oscillations in the flame front can occur.

The procedure adopted was to assume that the injection system is vibrating, thus establishing synchronized fuel flow modulation and then to derive, on the basis of a simple dynamic model, a formula for the resulting pressure variation.

Simplifying assumptions made in the model are as follows:-

(a) Shower-head injectors with low velocity jets, so that under vibration the break-up is into uniformly sized drops.

One thus has waves of drops entering the combustion zone.

In practice, of course, the jet is shattered into droplets and discrete drops are replaced by concentrations (bunches) of droplets. Dynamically, the situations are similar.

(b) The oxidiser, say liquid oxygen, is vaporised much more rapidly than the fuel. Hence fuel injection only is considered of significance in this work.

(c) All flow is axial.

(d) Only the longitudinal mode of instability will be specifically involved.\*

The full details of this initial work may be found in ref.8. The model was a very crude analogy, in which the pressure variation following the injection of one 'wave' of fuel drops into the combustion zone is equated to the time response of a linear second order system following an impulse-type disturbance. The equation for pressure as a function of time was

$$P = K \left\{ \exp(-\zeta \omega_n t) \frac{\zeta}{\sqrt{\zeta^2 - 1}} \sinh[\omega_n t \sqrt{\zeta^2 - 1}] \right\}$$

where  $P$  = instantaneous combustion pressure  
 $\zeta$  = damping ratio  
 $t$  = time  
 $K$  = constant (a function of the specific chamber, fuel/oxidant ratio etc.)

Expressions for  $\zeta, \omega_n, K$  in terms of system parameters were derived. These parameters were the combustion time lag and residence time of the gases in the chamber.

The intersection of the pressure variation for successive 'waves' leads to the high frequency combustion pressure variation as illustrated in Figure 1. Variation of frequency with injector-pressure drop is shown in Fig.2.

### Conclusions

This initial crude analysis was sufficient to demonstrate that if fuel flow modulation can be produced in the frequency range known to be associated with the phenomenon of high frequency combustion instability, then a large amplitude pressure variation will result.

It thus became essential as a next step to establish whether or not injector plate vibration could produce this flow modulation. As mentioned previously, most of the work on this grant has involved the investigation of fluid flow thro' injectors in the presence of mechanical vibration. This will be reported in Part 2.

**FIG.1** CHAMBER PRESSURE VARIATION WITH TIME  
INJECTOR PRESSURE DROP = 50 p.s.i.

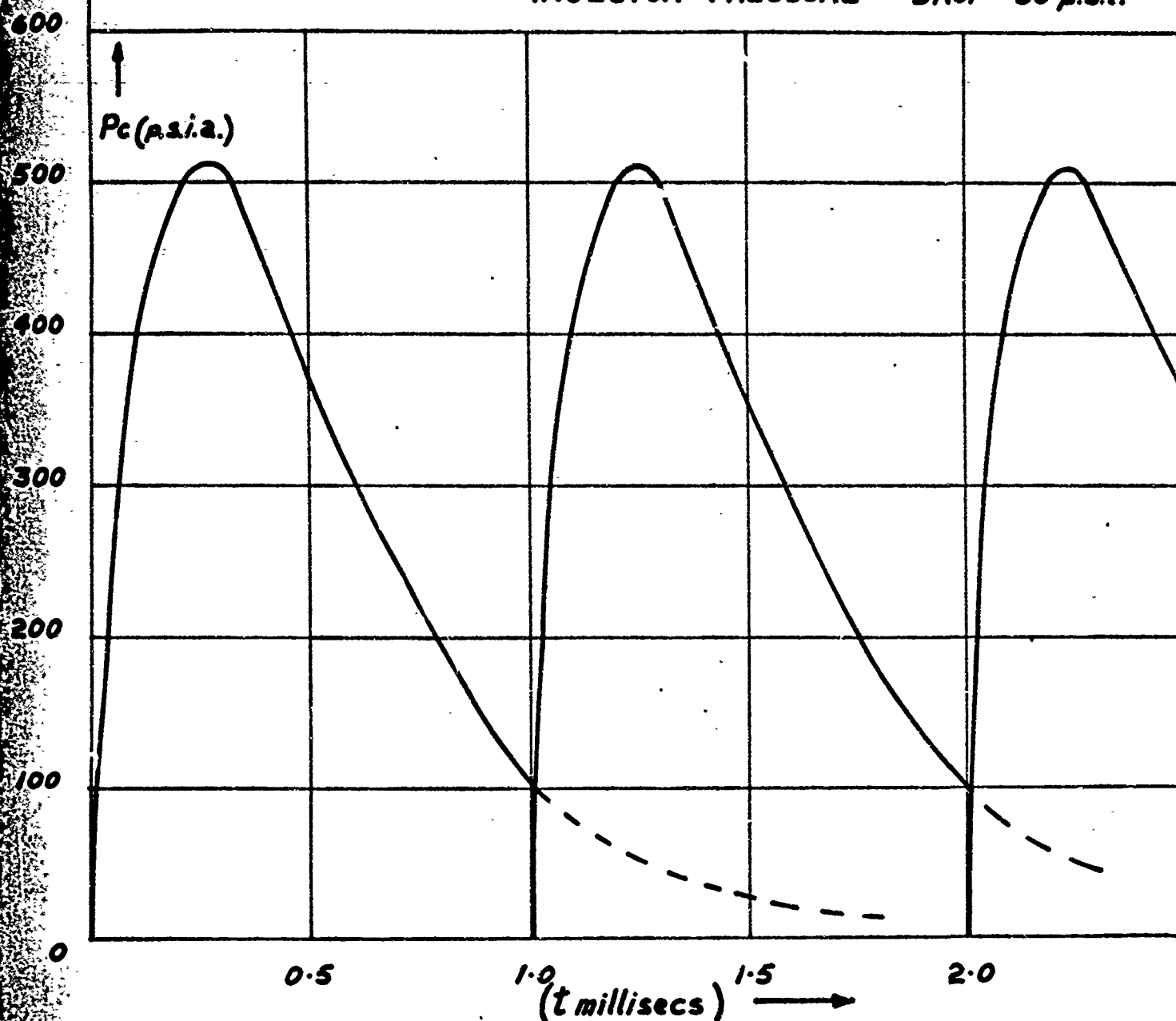
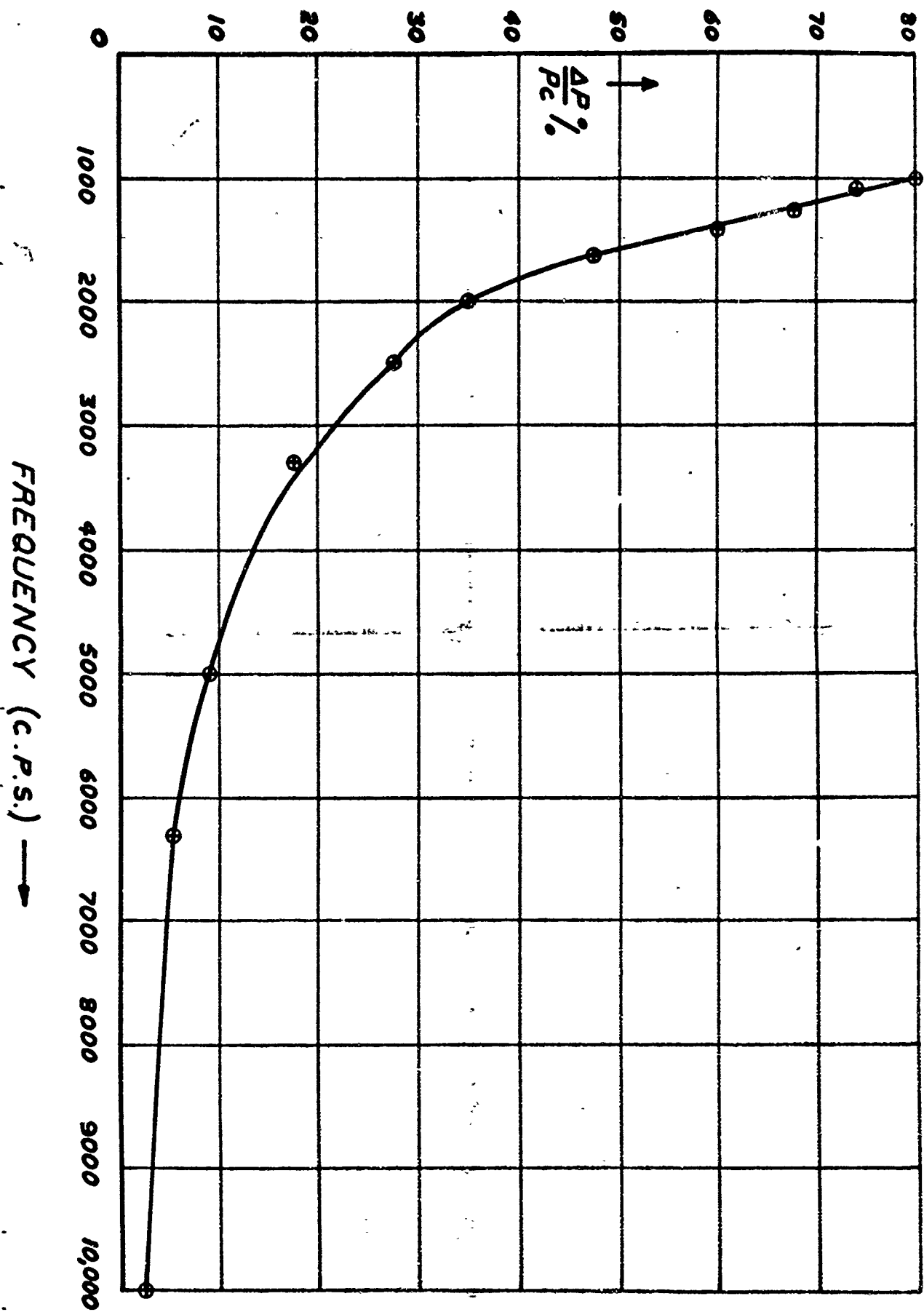


FIG. 2

MAGNITUDE OF PRESSURE VARIATION VS. VIBRATION FREQUENCY



Part 1. Appendix 1

Rocket Engine Noise and Structure Response

It is well known that the most important source of vibration in a rocket in a static test or during the powered subsonic part of flight, is the sound field of the rocket engine.

The noise of the engine has its origin in the very intense turbulence created in the shear layer when the fluid exchanges momentum with the atmosphere and has a much greater effect than direct vibration transmission from the engine.

The turbulent sound producing gas extends downstream from the nozzle, and two distinct regions may be identified in this extended source.

(a) the "near field" region within a wave-length or so of the nozzle, including not only outwardly propagating waves, but also reciprocating motions and pressure fluctuations.

(b) the "far field" where only radiated sound (representing energy abstracted from the jet) is involved and where the pressure fluctuations fall off as  $1/\text{distance}$ .

Work carried out on the near-field effects over the vehicle surface <sup>(1)</sup> indicate that they are small (at least for frequencies above 500 cps) and so from the point of view of structure response, it is only the far-field which is of interest.

Lighthill <sup>(2)</sup> has demonstrated that the radiation of sound by turbulence is caused by a volume distribution of quadrupoles - lateral or longitudinal. The noise field along the vehicle surface will only involve the longitudinal quadrupoles.

Measurements of the sound radiated by rocket engines <sup>(3)</sup>, show that the ratio of sound power to mechanical power is a constant, independent of the exhaust Mach number, the value being in the region of  $10^{-2}$ . In fact the  $V^8$  relation predicted by Lighthill reaches a saturation point somewhere between the jet and rocket engines.

The dimensionless spectrum function for rocket engines, based on experimental measurements is shown in Fig.3. It is to be noted that the spectrum is wide.

For a Strouhal number of unity, with a medium engine of 3 feet diameter, 140,000 lbs thrust and 7,000fps exhaust velocity, the frequency would be 2,300 cps and spectrum function  $A(f) = 1.1$ .

The spectrum function is proportional to the power per unit bandwidth and corresponds to a spectral density of  $5 \times 10^{-4} (\text{lbs/sq.ft})^2 \text{ c.p.s.}^{-1}$

The mean surface sound pressure would be about 50 lbs/sq.ft.

The total noise power in the above unit would be in the region of five million foot-pounds per second.

FIG.3.

SPECTRUM FUNCTION OF ROCKET ENGINE  
NOISE OVER MISSILE SURFACE

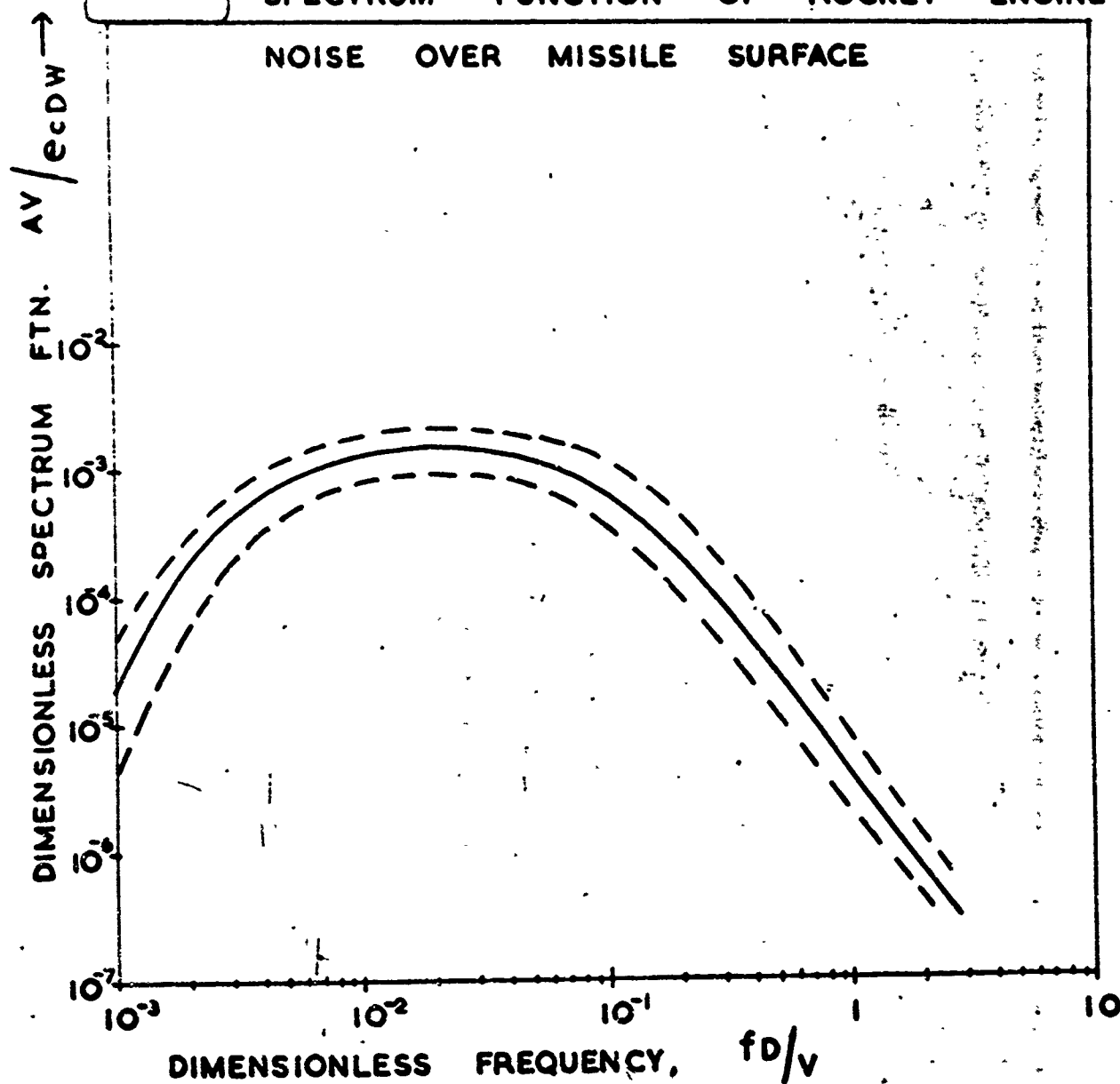


FIG. 4

SPECTRUM AMPLIFICATION FACTOR VERSUS  
MISSILE MACH NUMBER .

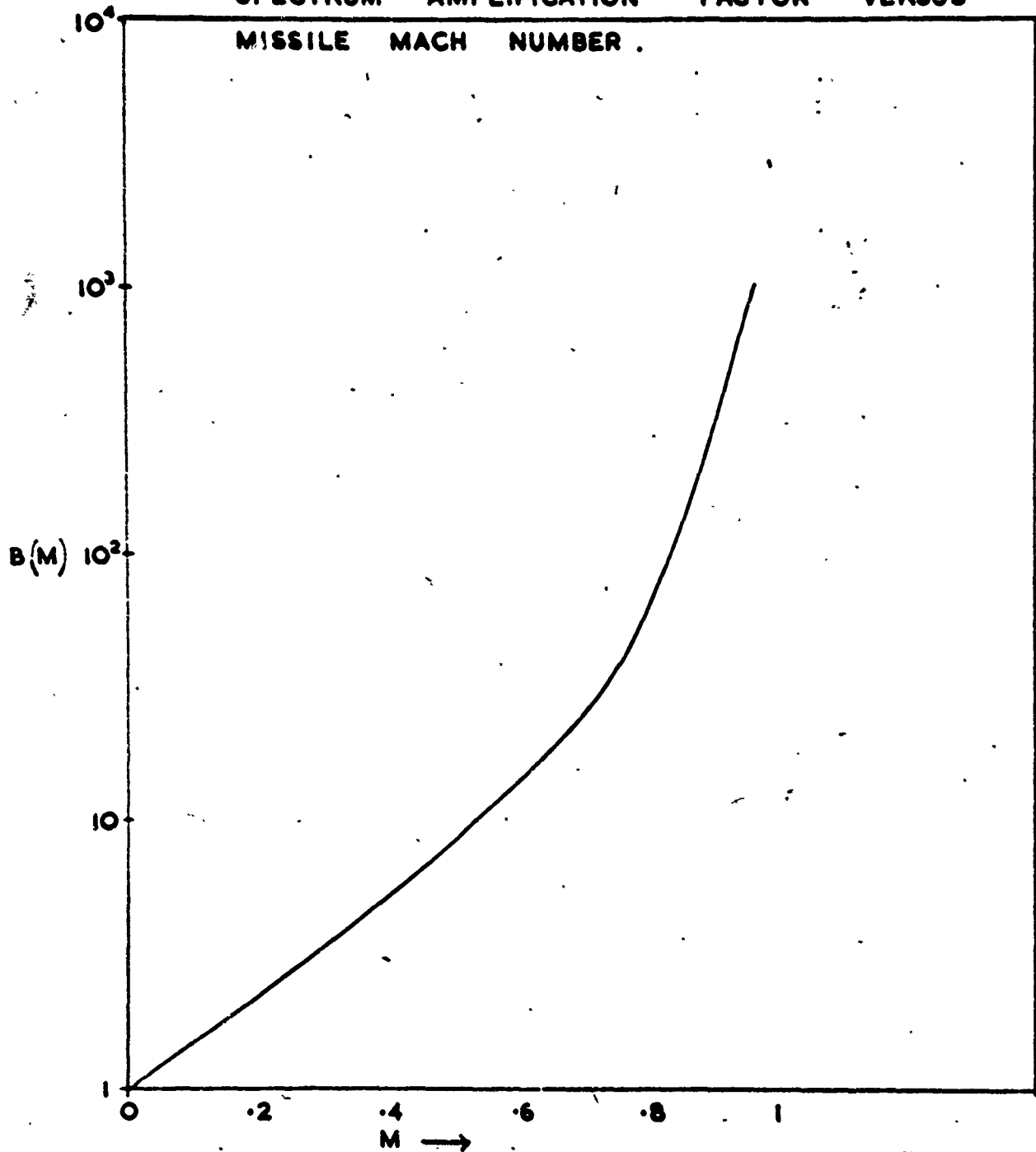
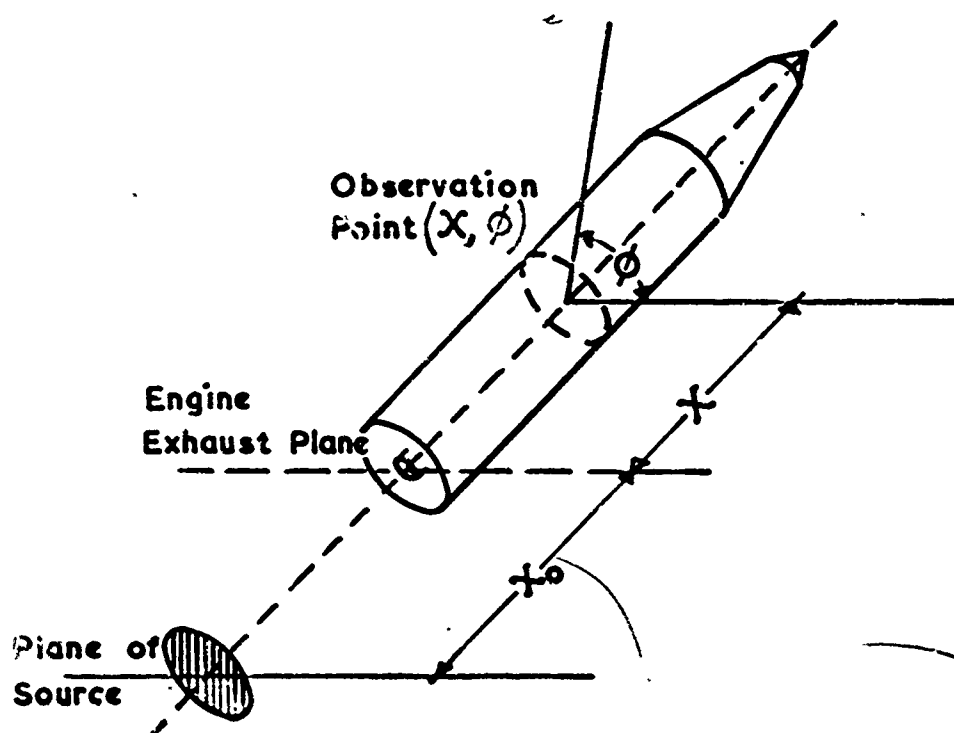


FIG 5

COORDINATE SYSTEM FOR ROCKET,  
NOISE SOURCE



### Effect of Missile Motion

There are two known major effects:

(a) the radiated power increases with the rocket velocity. Lighthill has shown that the differential power radiated in the forward direction by longitudinal quadrupoles is increased by the factor,

$$1/(1 - M)^6 \text{ where } M = \text{rocket Mach number.}$$

The engine noise field along the vehicle surface will tend to become very large as  $M$  approaches unity. The increase is limited, however, as it becomes increasingly difficult to excite vehicle vibrations as  $M$  approaches unity, because the effective sound wave length is reduced by the factor  $(1-M)$ .

In fig. 4 a graph of  $M$  versus spectrum function amplification factor,  $B(M)$ , is shown.

(b) the directivity pattern turns more towards the direction of motion.

Certainly then, the vehicle motion leads to an appreciable increase in the noise field at the structure surface.

### Response of the Vehicle Structure to the Noise Field

As long as the rocket Mach number is below unity, the sound generated in the far field (this may be centered 40 ft or so downstream from the nozzle) can reach the vehicle surface.

Only large structural response is of interest and so two particular cases need be considered:

- (i) Resonance - which occurs when the frequency of the exciting force equals a natural frequency of the structure. The noise spectrum being a wide one, all vehicle resonances can be excited.
- (ii) Modal Equivalence - which occurs when the sound wave-length (or speed) is equal to the wave-length (or speed) of free flexural vibrations in the structure <sup>(4)</sup>

The sound speeds involved range over a relatively narrow band from the sound velocity,  $c$ , to zero, for rocket Mach number ranging from 0 to 1, and so modal equivalences will be rare.

The largest vibration response will occur for those situations where both resonance and equivalence coincide, and thus those resonances with a wave-length equal to a noise field wave-length are of maximum interest. Such occurrences may be called Coincidences.

Crandall <sup>(5)</sup> has developed a step-by-step approach for determining these most important structural responses. He introduced circumferential modes to describe the angular variation of both the sound pressure and the induced vibration.

If  $w$  represents the flexural (radial) displacement of the structure surface, the vibration acceleration is  $\ddot{w}$ , and

$$\ddot{w} = \int_0^\infty \Phi(f) df$$

where  $\Phi(f)$  is the acceleration spectral density. The displacement,  $w$ , is represented by a Fourier series:

$$w(x, \phi, t) = \sum_{n=0}^{\infty} w_n(x, t) \cos n\phi$$

where the co-ordinate system  $(x, \phi)$  is as shown in Fig.5, and  $n$  is the circumferential order number.

The  $n = 0$  mode corresponds to expansion and contraction of the cylinder cross-section

$n = 1$  mode corresponds to translation of the cross-section

$n \geq 2$  modes correspond to bending or corrugation of the cross-section perimeter.

In circumferential modes the sound pressure,  $p$ , is written similarly as

$$p(x, \phi, t) = \sum_{n=0}^{\infty} p_n(x, t) \cos n\phi$$

The task is to express the acceleration spectral density,  $\Phi(f)$  in terms of the mean square-pressure spectral density.

It turns out that for pressurized cylinders there is only one circumferential mode of importance for low frequencies - the  $n = 1$  mode.

For higher frequencies ( $> 1000$  cps say) all modes are important and behave identically.

It also appears that coincidences can only occur for vehicle Mach numbers up to about 0.7.

Calculations on hypothetical rocket vehicles of the 140,000 lb thrust category, show that coincidences can occur during the early part of the flight (or in static test) and that

- (a) the frequencies fall in the range from 1,000 to 10,000 cps
- (b) rms accelerations up to 40g are possible.
- (c)  $n = 0, 1$  &  $\geq 2$  modes are possible.

Luperi and Tick (6) have recently reported work on vibration and unstable combustion in the L<sub>2</sub>99 engine. Acoustic pressure oscillations induced resonance in the engine mounting structure, resulted in build-up to vibration accelerations as high as 400 g. Even with isolators installed, values of 150 g were obtained.

Associated with these vibrations, a great increase in the magnitude of the combustion pressure oscillations occurred. This was ascribed by the authors as possibly being connected with the effect of mechanical vibration of the injection system.

It is contended in this work that the initiating mechanism for all forms of high frequency instability in liquid fuel rocket engines, can be traced to the massive mechanical vibration of the injection system driven by the intense sound field arriving at the vehicle surface.

**FIG.3 BREAK-UP LENGTH VS VIBRATION AMPLITUDE**  
**LOW FREQUENCY REGION**

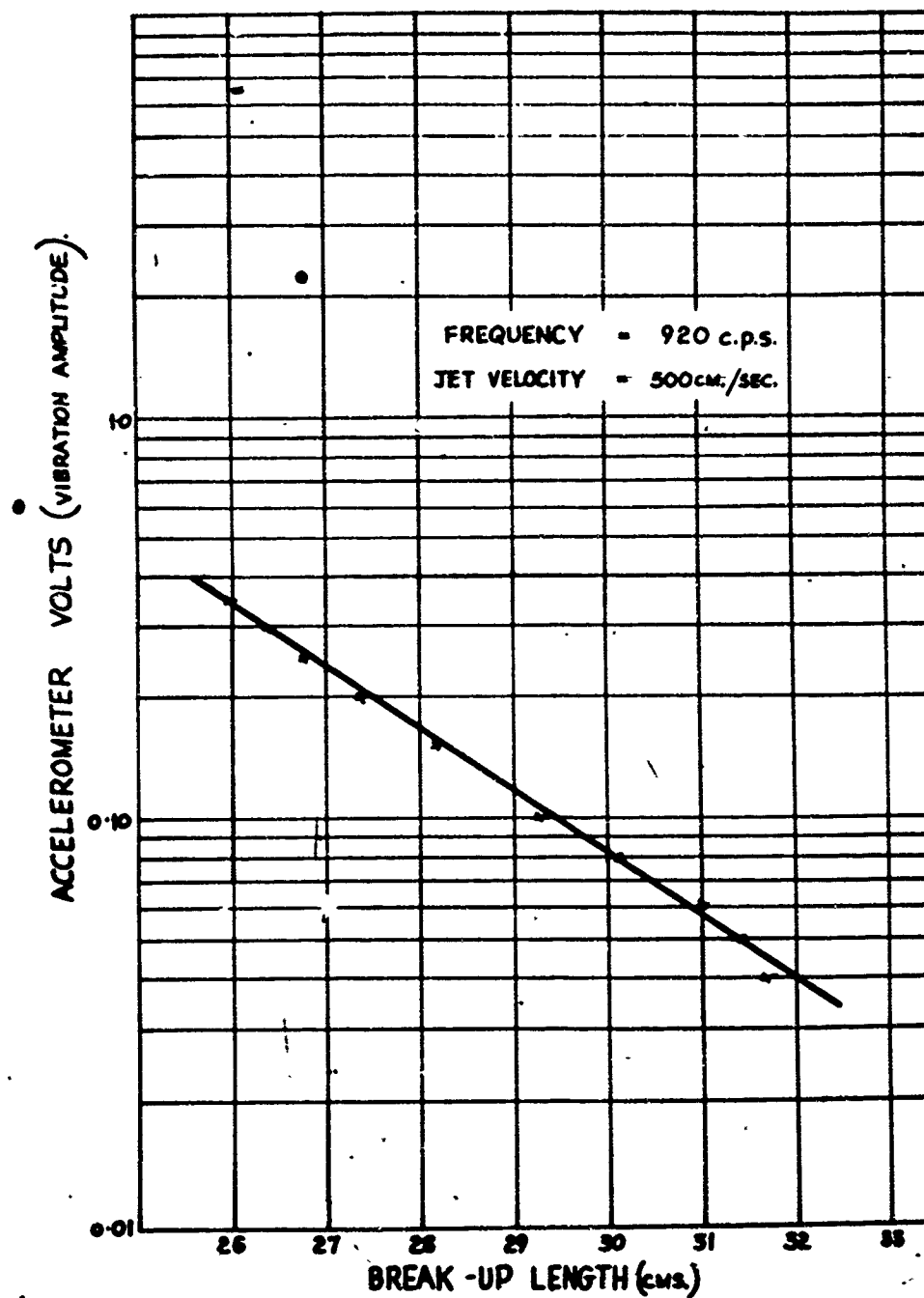


PLATE  
4.

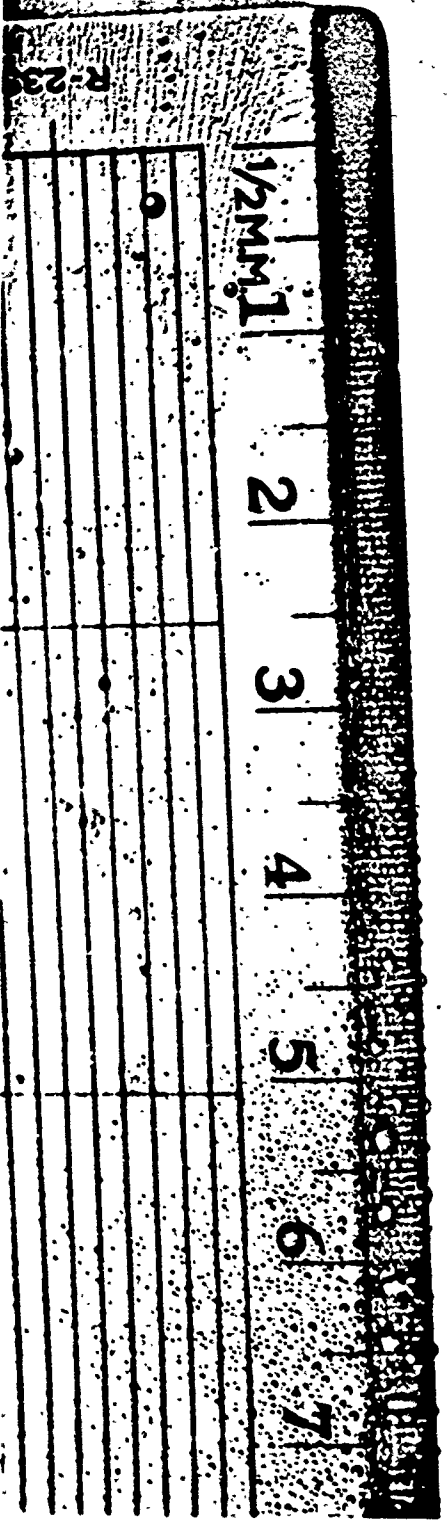


PLATE  
5.

1/2MM.1

2

3

4

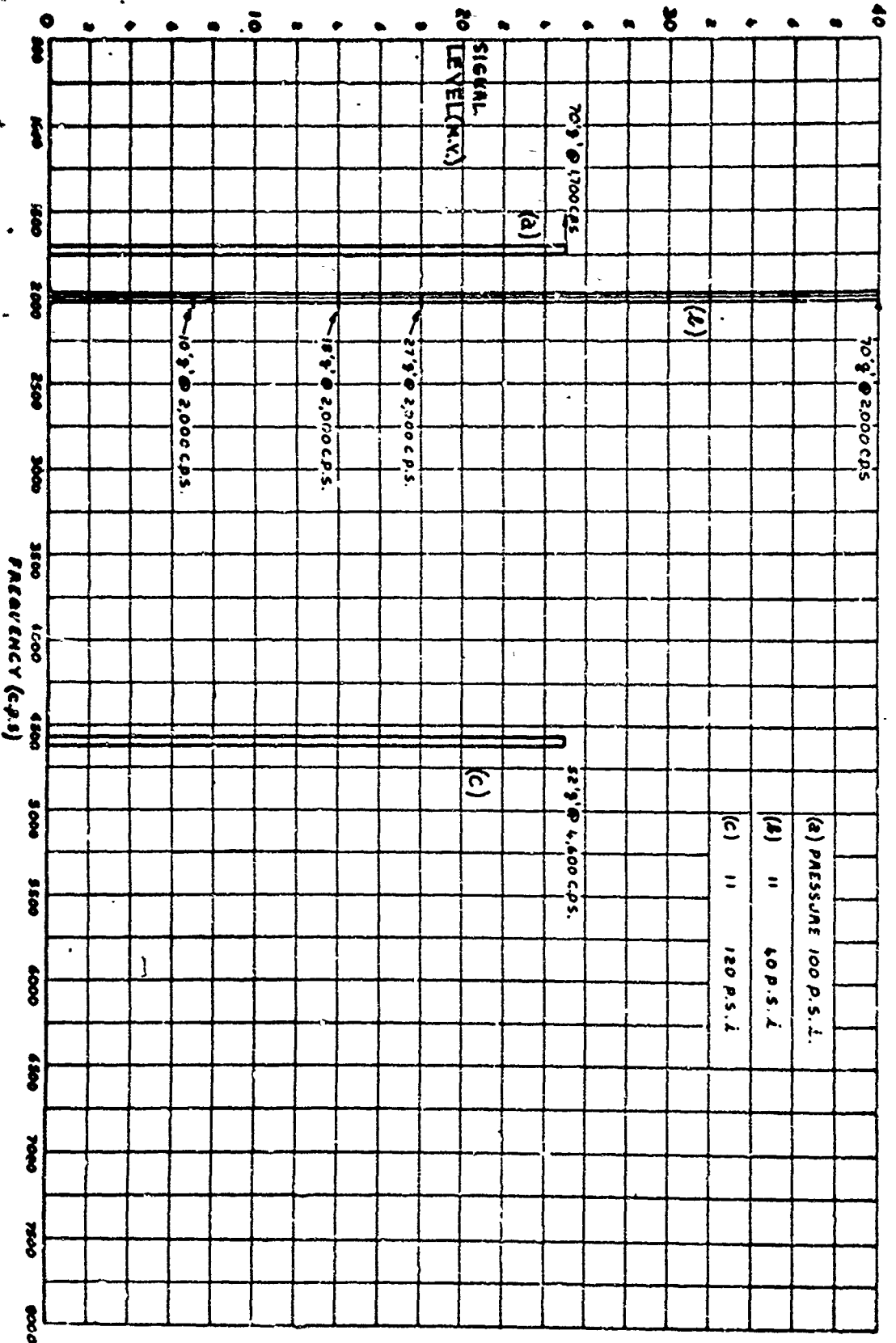
5

6

7

FIG. 9

WAVE-ANALYSER RESULTS



REFERENCES:

1. "Inherent Stability of Combustion Process", Pickford, R.S. and Peoples, K.G. A.R.S. 15th Annual Meeting, Washington, D.C. (1960).
2. "One-Dimensional Theory of Liquid Fuel Rocket Combustion" Spalding, D.B. Aero Research Council, C.P. 445, May (1958).
3. "Propellant Vaporization as a Design Criterion for Rocket Engine Combustion Chambers" Priem, R.J. and Heidman, R.F. NASA Tech. Rep. R-67 (1960).
4. Luperi, M.G., Tick, S.G. Detonation and Two Phase Flow (Academic Press, 1962), p. 321-338.
5. Dyer, G., Random Vibration (John Wiley & Sons, New York, 1958), Chapter 9.
6. von Gierke, H., Handbook of Noise Control Ch.23 McGraw-Hill (1957)
7. "On the Stability of a Plane Wave Front in Oscillating Flow" Markstein, G. & Squire, W. Journal of the Acoustical Society of America Vol. 27 No. 3 (1935) p.416.
8. "A Driving Mechanism for High Frequency Combustion Instability in Liquid Fuel Rocket Engines" P.D. McCormack, Journal of the Roy. Aero. Soc. P.633. Sept. 1964.

Part 2.

An Experimental and Theoretical Analysis  
of Cylindrical Liquid Jets Subjected  
to Vibration.

Notation:-

- $\alpha$  = the expansion of the jet surface
- $\beta$  = a constant
- $\rho$  = liquid density
- $T$  = surface tension
- $a$  = position of the jet surface
- $k$  = wave number of disturbance on jet
- $\lambda$  = wave-length " " " "
- $q$  = exponential build-up factor
- $\eta$  = liquid viscosity
- $g$  = acceleration due to gravity (32.2. ft/sec<sup>2</sup>)
- $z$  = ordinate along jet axis
- $r$  = jet radius
- $\phi$  = velocity potential
- $u$  = axial jet velocity
- $v$  = radial " "
- $A$  = constant
- $u'$  = modulation velocity
- $u_0$  = background modulation velocity
- $\omega$  = angular velocity =  $2\pi f$
- $f$  = frequency
- $P$  = potential energy of jet per unit length
- $K$  = kinetic energy of jet

### Section 1. Introduction

The authors have reported initial experimental work on the effects of mechanical vibration on the break-up of a laminar cylindrical water jet in air.

Results were compared with the 1st order theory developed by Lord Rayleigh <sup>(2)</sup>. He had shown that a cylindrical liquid jet could be triggered into instability by small rotationally symmetric disturbances, provided the wave-length on the jet was greater than the jet circumference.

C. Weber <sup>(3)</sup> carried out a similar analysis, and extended it to include the effect of viscosity and an estimate of aerodynamic effects at the higher jet velocities. (above about 15 metres/sec).

No attempt was made, however, to specify the physical nature of the initiating disturbance, nor to extend the analysis to the case of finite driving amplitudes. In this work both of these points will be covered. The equation of free motion obtained by Rayleigh was as follows:-

$$\frac{d^2 \Delta}{dt^2} + \frac{T}{\rho a^3} \cdot \frac{j k a J_0'(j k a)}{J_0(j k a)} (k^2 a^2 - 1) \Delta = 0$$

----- (1-1)

As  $\Delta \propto e^{q \cdot t}$  then

$$q^2 = \frac{T}{\rho a^3} \cdot \frac{j k a J_0'(j k a)}{J_0(j k a)} \quad (1-2)$$

where  $q$  is the exponential build-up factor.

Weber extended this analysis to cover viscous effects and the amplifying aerodynamic suction effect. He obtained the following equation for  $q$ :

$$q^2 + q \cdot \frac{3\eta k^2}{\rho} = \frac{T}{2\rho a^3} (1 - k^2 a^2) + \frac{\rho_{air} U^2}{2\rho a^2} \cdot k^3 a^3 \cdot \frac{j H_0''(j k a)}{H_1''(j k a)}$$

For relatively inviscid liquids such as water and paraffin the viscous correction can be ignored and by considering jet velocities below 1500 cm/sec the aerodynamic effects are small <sup>(3)</sup>. Moreover, as will be seen later, in the

presence of finite initiating amplitudes Weber's aerodynamic treatment (only applicable to sinusoidal corrugations) would have to be replaced by a more appropriate analysis.

The break-up and periodicity of liquid jets has been studied again recently. This stimulus is due to possible connection with the phenomenon of combustion instability in liquid rocket engines. It was found <sup>(4)</sup> <sup>(5)</sup> that the Rayleigh-Weber capillary type instability could be driven by subjecting the liquid jet to sound fields. Very small pressure variations and low frequencies were used ( $\pm 0.5$  psi and 200 cps) and the results were unspectacular and limited to low velocity laminar jets.

Reba and Brosilow <sup>(6)</sup>, however, extended this work to large pressure variations. The jet entered a chamber which effectively had a reciprocating piston at one end. The pressure downstream of the injector was varied from 5 to 30% of the steady pressure at frequencies up to 3,000 cps. Pronounced periodicity was induced on the jets (oil and water). Considerable quantitative investigation, such as the effects of oscillation frequency and amplitude, injector hole size, etc. was carried out.

Reba and Brosilow postulate a mechanism based on flow modulation caused by the pressure variation downstream of the injector hole. They ascribe the corrugations on the jet as due purely to the resulting "bunching" action of the liquid in the jet. (bunching is a term used to denote the radial velocity of liquid due to the relative velocity of adjacent particles in the jet).

Arbitrarily they ignored capillary action, but for the low initiating amplitudes obtained, as evidence by the sinusoidal type of build-up on the jet surface, it was unjustified. This is characteristic of predominant capillary action.

Their analysis considered the effect of the resistance and inertance of the fluid in the orifice cavity on the flow modulation, and analytical formulae predicting jet length to the "first thickening" were derived. Again, this distance criterion is hypothetical as 'bunching' is a continuous process (till de-bunching starts).

It will be seen later that Reba & Brosilow would have been more correct in their assumption of predominant "bunching" at much higher velocity modulation values. It is doubtful, however, if such values could be achieved by reasonable pressure variations downstream of the injector. It is the pressure upstream which fixes the discharge velocity and the downstream pressure waves must propagate upstream and in doing so their effect is enormously attenuated.

In this respect injector vibration is more efficient in that it appears to induce pressure variations directly upstream of the injector hole (see Section 11).

Thus, the only theoretical analysis of significance in this field has been that of Rayleigh and Weber and is restricted to 1st order effects and infinitely small initiating amplitudes. With the latter restriction, of course, the flow modulation merely serves as a trigger, liquid bunching is negligible, and capillary type instability predominant.

It was the objective of this work to produce a theory which (a) will cover second order effects (i.e. will extend to appreciable corrugation sizes); (b) that will include the capillary effect and the 'bunching' effect. The latter must be considered when the initiating amplitude (velocity modulation) is of finite magnitude and will become predominant at large initiating amplitudes.

The first analysis (Section 11) to be presented

will merely extend the Rayleigh theory to second order effects, but will include the velocity modulation as the initiation for the instability (that is, restriction to very small velocity modulation is made).

The second analysis not only extends the treatment to second order effects, but includes the 'bunching' effect and so attempts to bridge the transitional gap between predominant capillary action and predominant liquid 'bunching' action.

## Section 2. Experimental Background

The main experimental results reported here are an extension of the work previously reported by the authors <sup>(1)</sup>.

Briefly it covers

(a) the results obtained at much higher vibration acceleration values (up to above 300 g).

(b) the repeating of break-up length versus initiating vibration amplitude measurements for paraffin and comparison with the water results. It is assumed that the induced velocity modulation is proportional to vibration amplitude.

(c) the detection of pressure fluctuations in the cylindrical chamber behind the injector.

Details of most of the apparatus used has been given in Reference 1.

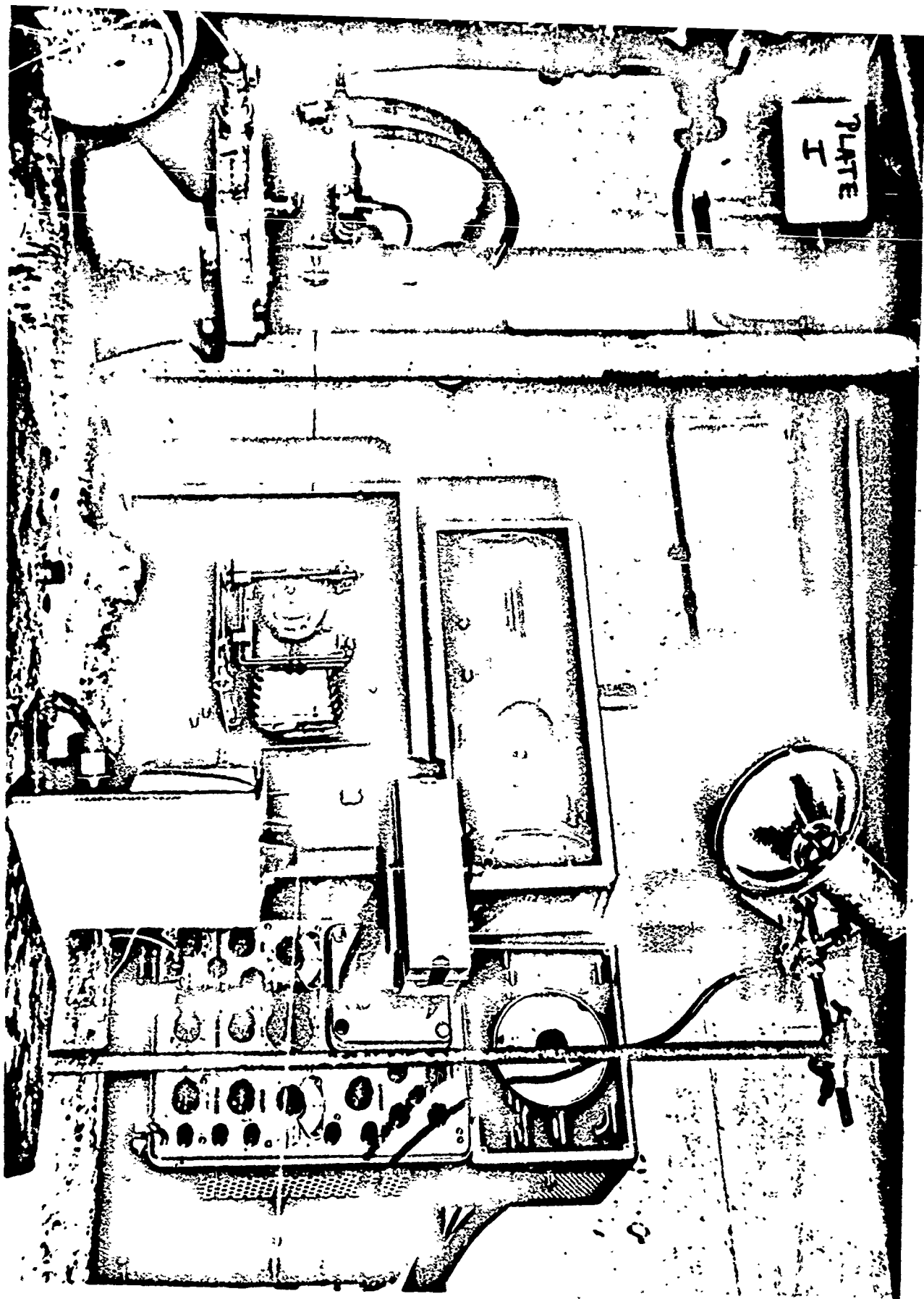
Previous results may be summarized as follows:-

For a laminar water jet subjected to modulation driving amplitudes corresponding to vibration acceleration values of up to 20 'g', the graph of breakup length (or time) followed reasonably closely that predicted by the Rayleigh-Weber theory. However,

(i) using an experimentally determined discharge coefficient to get the true initial jet radius following contraction, estimates of the build-up factor,  $q$ , indicated a value of about 300. This is significantly higher than the value of 225 expected on the Rayleigh-Weber theory.

(ii) the graphs of instability build-up versus jet length (or time) revealed considerable departure from the purely exponential characteristic inherent in the Rayleigh analysis.

As mentioned before, the slightly peaked appearance of the corrugations at vibration acceleration values of about 20 'g'.



GENERAL VIEW OF APPARATUS

was interpreted as an indication that velocity modulation is at work. At low acceleration values this modulation is very small and acts only as a trigger for the Rayleigh capillary type instability. At higher values and thus stronger modulation, liquid bunching along the jet would become appreciable.

To investigate this further, vibration values up to about 250 'g' were applied to the cavity behind the injector. Typical results for water and paraffin are shown in Plates II. and III. The jet velocity was 45 fps, and the vibration frequency 2,000 cps.

Disc formation close to the injector is the extraordinary result. The paraffin discs are more affected by aerodynamic effects, being bent and atomized round the edges. This is probably due to paraffin having a much smaller surface tension than water.

The bulges between the discs (in the case of water) is due to the build-up of harmonics of the applied vibration on the cylinders joining the discs.

The disc formation is striking confirmation of the velocity modulation mechanism.

It is obvious that the Rayleigh-Weber theory could not be expected to cover this situation.

A satisfactory theory for finite initiating amplitudes (velocity modulation) must include both capillary and bunching effects.

Graphs of break-up length versus log (vibration amplitude) for paraffin and water jets at a velocity of 1.5 metres/sec are shown in Fig.1. Note: the ordinate scale is in accelerometer volts. This is proportional to vibration amplitude, in turn proportional to acceleration value. It is reasonable to assume (see discussion later) that the velocity modulation amplitude is linearly related to the 'g' value. Experimental

PLATE  
2.

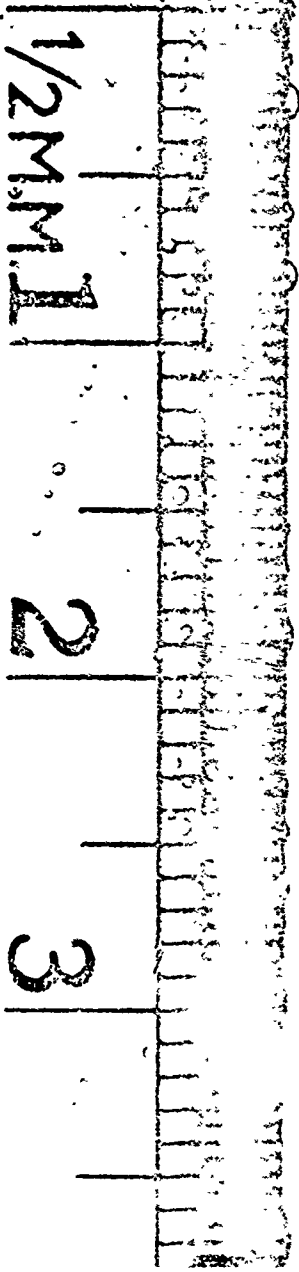


PLATE  
3.

1033

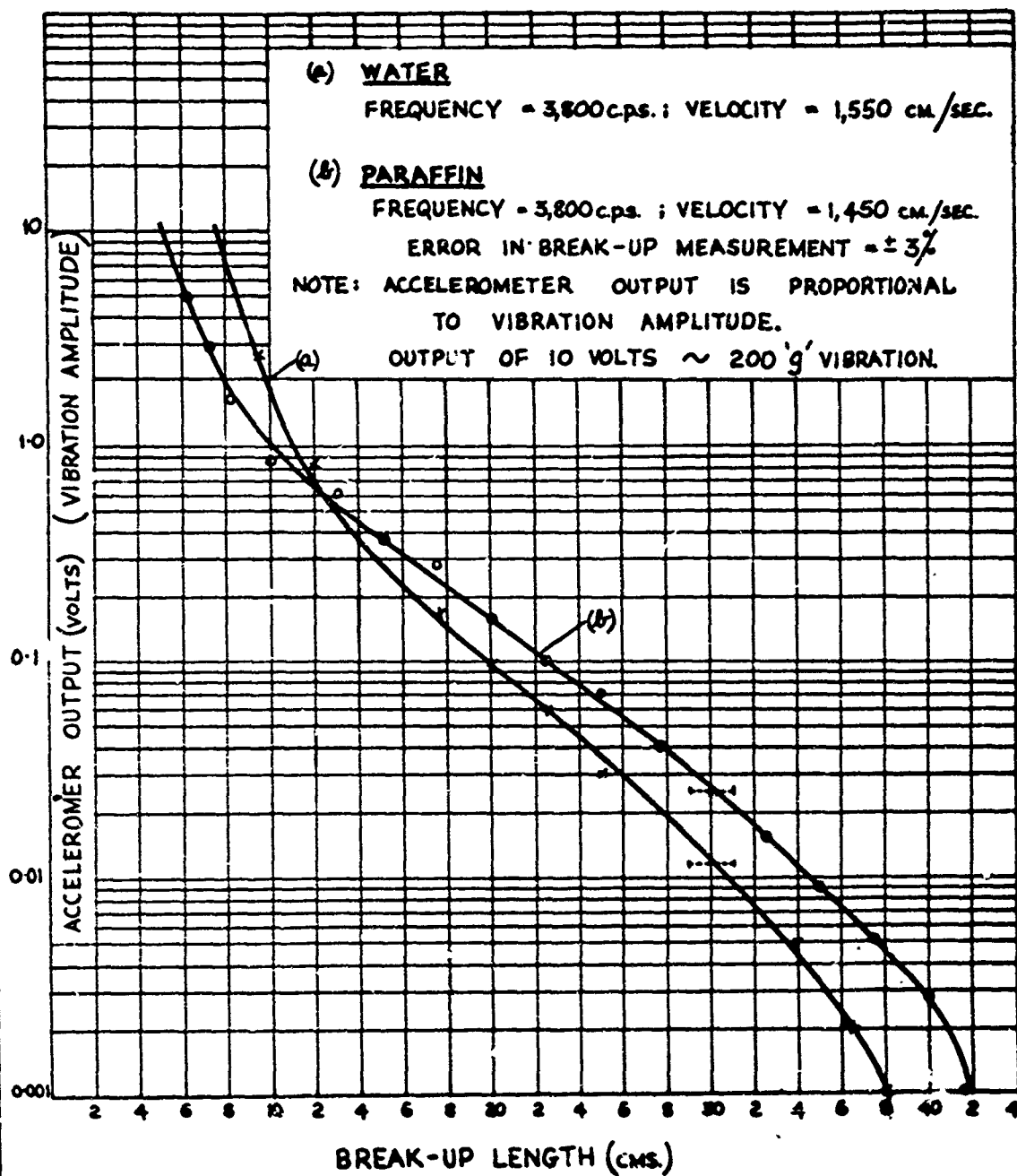
N

 $\omega$ 

4



**FIG.1 BREAK-UP LENGTH VS VIBRATION AMPLITUDE**  
EXPERIMENTAL



points were taken up to about 50 'g's of vibration ( about 3 volts accelerometer output).

The curves for water and paraffin are very similar. The cross-over point would indicate that for a given vibration, a larger velocity modulation value is induced in paraffin. As the effect is probably closely connected with the liquid elastic properties at high frequencies, one might expect this, as paraffin has a lower relaxation frequency than water and so a higher shear modulus of elasticity.

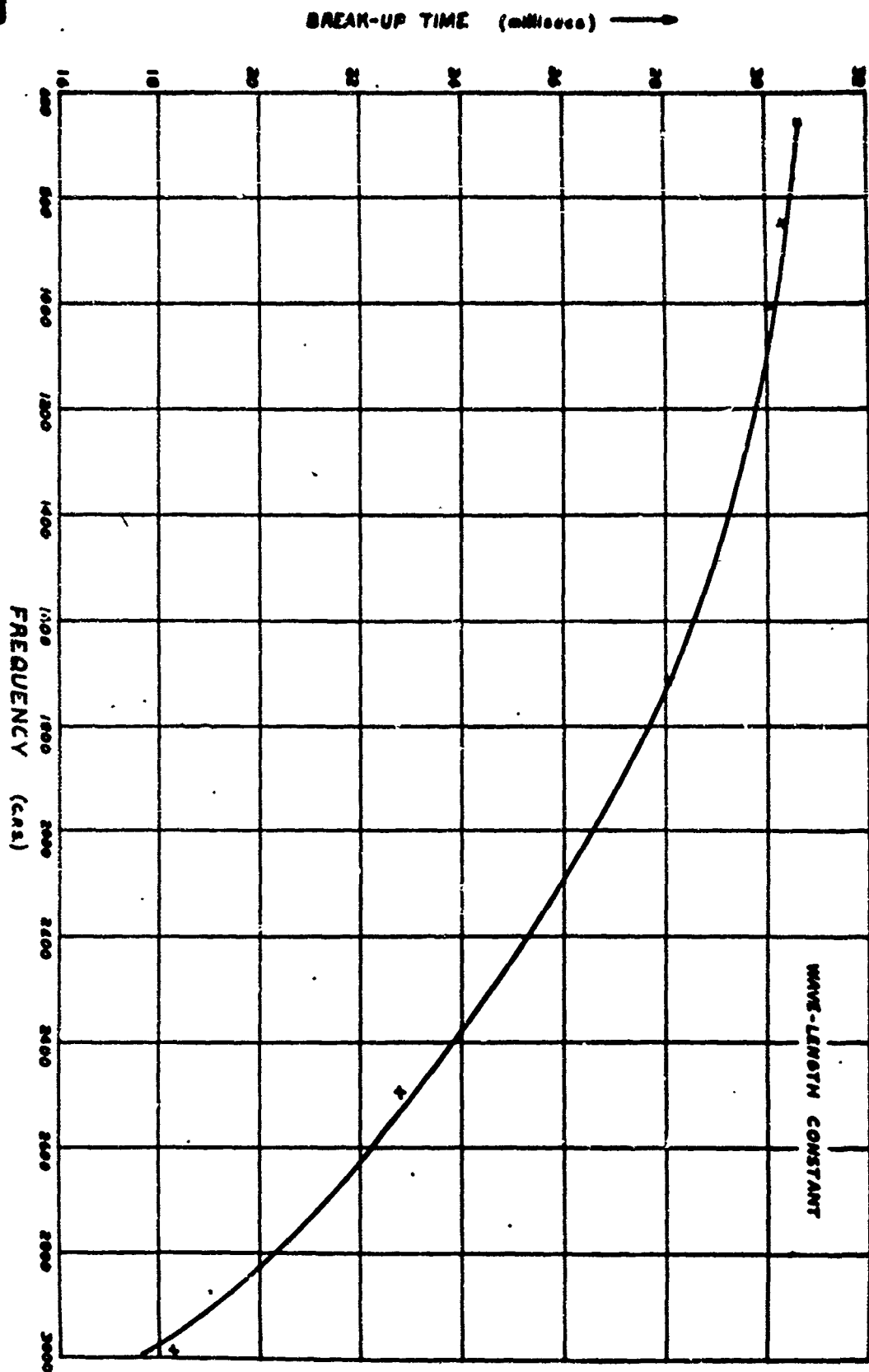
The curves theoretically should approach infinite break-up lengths at zero amplitude, but very small random effects (pressure fluctuations in the injector cavity) are always present and cause the finite limits observed in practice.

It is fairly obvious that there is no unique exponential build-up factor 'g'. However, by restriction to the range below about 1.0 volts (or 20 'g') an approximate q factor can be extracted and this is in effect what was done in our previous work.

An attempt was made to isolate the bunching effect (dependent on frequency) from the capillary effect (dependent on wave-length). A series of break-up length versus vibration frequency measurements was carried out, keeping the wave-length on the jet constant by variation of jet velocity. The resultant graph (for water) is shown in Fig.2 (break-up time has been used here). It is seen that above about 1,000 cps the break-up time decreases almost linearly with frequency (or acceleration value, as the amplitude was also held constant). Below about 1,000 cps vibration would have little effect on break-up. It is possible that this corresponds to a first relaxation frequency for water.

By the use of very small velocity modulation values it should be possible to simulate the infinitely small disturbance

FIG. 2 BREAK-UP TIME V. VIBRATION FREQUENCY - EXPERIMENTAL -



region. This was done by using a frequency of 1,000 cps, a jet velocity of 300 cm/sec and 'g' from 4 to 20. The resulting curve is shown in Fig.3. It is seen that a good straight line is obtained. A q value of 290 was obtained from this graph. It will be seen later (Section 3) that the difference between this and the value expected using Rayleigh's analysis is explained by taking 2nd order effects into account.

#### High Velocity Jets

Although the theoretical analysis will be restricted to laminar jets, one would expect that the strong liquid bunching produced with very high 'g' vibration, should have an effect on high velocity turbulent jets. This of course is the case most relevant to rocket engine combustors. That this is true can be clearly seen from Plates IV. and V. These photos are of water jets, from a 0.25 cm orifice. The velocities were 90 and 145 fps respectively, with vibration acceleration of about 200 'g' and at a frequency of 4,500 cps. The disc formation is still very evident, but ligament formation with subsequent break-up into droplets, tends to cloud the discs from view.

To prove that mass flow modulation was occurring even with high velocity jets, a focussed light beam was passed through the jet and on to a photo-electric cell. The output from the photo-cell was fed to a Marconi wave-form analyser and the spectrum in the vicinity of the applied vibration frequency examined carefully.

Up to the highest pressures possible (about 150 p.s.i. yielding a jet velocity of roughly 140 fps), a sharp peak in the analyser output was found at the applied frequency. The results are illustrated in Fig.9 (background noise has been subtracted out and was always at least an order of magnitude below the peak). One may conclude that vibration will induce appreciable mass flow modulation even with high velocity turbulent jets.

### Injector Cavity Pressure Fluctuations

Reba and Braslow reported that they detected no pressure fluctuations in the cavity behind the injector. As the mechanism of velocity modulation would involve pressure fluctuations upstream of the injector hole, an attempt was made to detect these using a high frequency Piezo transducer. This had a resolution of 0.015 psi, an upper frequency limit of over 10,000 cps but was designed for a pressure range of up to 200 psi (giving a 3 volt output).

The greatest difficulty lay in the fact that the transducer was slightly sensitive to the vibration and all readings had to be subtracted from a background level taken with no liquid in the cavity. Also maximum vibration acceleration values of only up to about 25 'g' were safe.

The results were thus not conclusive but did indicate that an effect (or signal) was obtained only when the transducer was mounted on the front plate of the injector cavity - perpendicular to the direction of vibration. A signal to noise ratio of 2:1 was obtained, the following numerical results being recorded:

Vibration 'g' : 25

" frequency: 4,500 cps

Output signal (from Piezo amplifier) = 0.032

" " frequency = 4,500 cps

The signal represented a pressure variation of  $\pm 2$  p.s.i., or  $\pm 5\%$  of the static pressure in the cavity.

Projection of the transducer face  $1/4$ " beyond the plate surface resulted in zero signal again.

The production of shear waves in the boundary layer along a plate oscillating in its own plane is well known and has been studied by Glauert <sup>(7)</sup>, Schlichting <sup>(3)</sup> and others.

Further work, theoretical and experimental, on the effect of vibration on the hydrodynamics of the injector cavity will

be well worthwhile. It will be tentatively postulated here that shear waves produced by the vibration, at the injector plate, can propagate across small injector holes and thus cause velocity modulation in the emerging jet.

### Section 3. Theoretical Analysis of Jet Instability for Very Small Velocity Modulation Amplitudes.

Consider a frame of reference moving with the mean jet velocity. With axial symmetry, the two co-ordinates of the system are  $r$ , the radius, and  $z$  along the jet axis.

The surface of the jet at any instant  $t$ , is given by

$$r = a + \mathcal{L} \quad \text{-----} \quad (3.1)$$

where  $a$  is the radius of the undisturbed jet, and  $\mathcal{L} = \mathcal{L}(z, t)$  is the build-up. It will be considered initially that  $\mathcal{L}$  is small with respect to  $a$ .

As the motion is irrotational,

$$\nabla^2 \phi = 0$$

where  $\phi$  is the velocity potential and

$$u = \text{axial velocity} = -\frac{\partial \phi}{\partial z}$$

$$v = \text{radial velocity} = -\frac{\partial \phi}{\partial r}$$

The boundary conditions which  $\phi$  must satisfy are:

(i) the free surface condition, i.e. a particle on the surface will remain there.

Consider a quantity,

$S = a + \mathcal{L} - r$ . This is a quantity which varies from particle to particle, but for a particle on the surface  $S = 0$ .

Thus, on the surface,  $\frac{dS}{dt} = 0$ , which is differentiation following the motion of the fluid. It can be written in partial derivatives as,

$$\frac{\partial S}{\partial t} + \frac{\partial S}{\partial z} \cdot \frac{dz}{dt} + \frac{\partial S}{\partial r} \cdot \frac{dr}{dt} = 0$$

or

$$\frac{\partial S}{\partial t} + u \cdot \frac{\partial S}{\partial z} + v \cdot \frac{\partial S}{\partial r} = 0$$

In terms of  $\mathcal{L}$  this yields the equation corresponding to the free surface boundary condition.

$$\frac{\partial \mathcal{L}}{\partial t} + u \frac{\partial \mathcal{L}}{\partial z} - v = 0 \quad \text{-----} \quad (3.2)$$

(ii) Bernouilli's equation

If  $p$  is the pressure in the jet, and  $\rho$  is the liquid density, this equation is

$$-\frac{\partial \phi}{\partial t} + \frac{1}{2}(u^2 + v^2) + p/\rho = \text{constant} \quad \text{-----} \quad (3.3)$$

On the free surface, a balance of forces gives

$$p/\rho = \frac{p_{atm}}{\rho} + T/\rho R \quad \text{-----} \quad (3.4)$$

where  $R$  is the jet radius of curvature

$T$  " " " surface tension

On the free surface, therefore, the following equation holds:

$$-\frac{\partial \phi}{\partial t} + \frac{1}{2} \left[ \left( \frac{\partial \phi}{\partial z} \right)^2 + \left( \frac{\partial \phi}{\partial r} \right)^2 \right] + T/\rho R = \text{constant} \quad \text{-----} \quad (3.5)$$

This is the second boundary condition equation. It can be expressed in terms of  $\mathcal{L}$  by means of a tedious calculation, giving

$$-\frac{1}{R} = -\left( \frac{1}{R_1} + \frac{1}{R_2} \right) \div \left[ \frac{1}{a} + \frac{\mathcal{L}}{a^2} - \frac{\partial^2 \mathcal{L}}{\partial z^2} \right] + \left[ -\frac{\mathcal{L}}{a^3} + \frac{1}{2a} \left( \frac{\partial \mathcal{L}}{\partial z} \right)^2 \right] \quad \text{-----} \quad (3.6)$$

Terms in  $\mathcal{L}^3$  have been neglected.

First approximation

Neglecting terms in  $\mathcal{L}^2$ , we assume that  $\phi$  has the form

$$\phi = A \cdot e^{qt} e^{ikz} J_0(jkr) \quad \text{-----} \quad (3.7)$$

and this leads to the original Rayleigh expression for the exponential build-up factor  $q$ .

### Second Approximation

In this case, powers of  $\phi$  &  $\mathcal{L}$  must not be neglected. To extend the analysis to second order terms,  $\phi$  must include a term corresponding to the residual term,  $-\frac{\partial \phi}{\partial z} \cdot \frac{\partial \mathcal{L}}{\partial z}$ , in the boundary conditions. So for a second order analysis we assume

$$\phi = \phi_1 + \phi_2 = A e^{\eta t} e^{j k z} J_0(j k r) + \beta A^2 e^{2 \eta t} e^{2 j k z} J_0(2 j k r) \quad (3.8)$$

$\mathcal{L} = \mathcal{L}_1 + \mathcal{L}_2$  and  $\beta$  is a constant.

For  $r = a + \mathcal{L}$ , and writing the boundary conditions to a second order approximation, and taking the special case of  $k a = 0.5$  (centre of the Rayleigh spectrum), leads to the following expression for  $\phi$ ,

$$\phi = A e^{\eta t} e^{j(\frac{1}{2} \pi z)} J_0(\frac{1}{2} j) + A^2 \left( \frac{0.034}{q a^2} \right) e^{2 \eta t} e^{j(3/2 \pi)} J_0(j) \quad (3.9)$$

where  $q$  = Rayleigh build-up factor

$$= \frac{\pi}{2 e a^3} k^2 a^2 (1 - k^2 a^2) = \frac{3}{32} \cdot \frac{\pi}{e a^3} \text{ for } k a = 0.5$$

The equation for  $\mathcal{L}$  then becomes

$$\mathcal{L} = \frac{-A j}{2 \pi q} e^{\eta t} e^{j(\frac{3}{2} \pi)} J_0'(\frac{1}{2} j) + \frac{A^2}{2} \left( \frac{0.034}{q^2 a^3} \right) e^{2 \eta t} e^{j(3/2 \pi)} \quad (3.10)$$

A value for the constant  $\alpha$  may be obtained by applying the boundary condition (or initial condition) at the orifice. This will be a small velocity modulation  $u'$ , and

$$\left| \frac{\partial \phi}{\partial z} \right| = \text{modulation velocity} = u' = A/2 a \quad (3.11)$$

It is assumed that  $u'$  is known.

Hence

$$\mathcal{L} = \frac{-u'j}{q} e^{qt} e^{j(\frac{3}{2a})} \int_0^t (\frac{1}{2}j) + (2au')^2 e^{2qt} e^{j(\frac{3}{2a})} \left( \frac{.016}{q^2 a^3} \right) dt \quad (3.12)$$

As  $z = U \cdot t$  one can then either compute the build-up,  $\mathcal{L}$ , versus time, or the profile on the jet at successive intervals of time.

Equation (3.21) can be reduced to the following

approximate form:

$$\mathcal{L} = e^{qt} \left\{ \cos\left(\frac{3}{2a}\right) \frac{u'}{4q} + (2au')^2 \left( \frac{.016}{q^2 a^3} \right) e^{qt} \cos\left(\frac{3}{2a}\right) \right\} \quad (3.13)$$

A typical result for the profile on a water jet from a 0.12 cm injector is shown in Fig.4. The jet velocity was 1000 cm/sec and it was assumed that the applied vibration was producing a velocity modulation of  $u' = 5$  cm/sec. Fig.5 shows values of  $\mathcal{L}$  versus  $q \cdot t$  ( $t$  measured from  $t = 0$  at the orifice). As the build-up will be still closely exponential we can write

$$\mathcal{L} = \text{constant} \cdot e^{K(q \cdot t)}$$

where  $(q \cdot t)$  is the independent variable.

From the graph a value of  $K = 1.5$  was determined and so an effective 'q' factor of 330 was arrived at.

This value agrees quite well with the experimental estimates of  $q$  reported in the previous paper <sup>(1)</sup>.

It is interesting to note that

$$a \sqrt{\frac{T}{2ea^3}} = \sqrt{\frac{T}{2ea}} \quad \text{and so has the dimensions}$$

of velocity. For the injector used and with water as the liquid, this characteristic velocity turns out to be about 50 cm/sec.

Now,

$$\frac{A}{q a^2} = \frac{2 u'}{\frac{\sqrt{3}}{4} a \sqrt{\frac{T}{2ea}}} = \frac{8}{\sqrt{3}} \cdot \frac{u'}{\sqrt{\frac{T}{2ea}}} \quad (3.14)$$

FIG. 4 SOME PROFILES OF BUILD-UP ALONG LIQUID JET

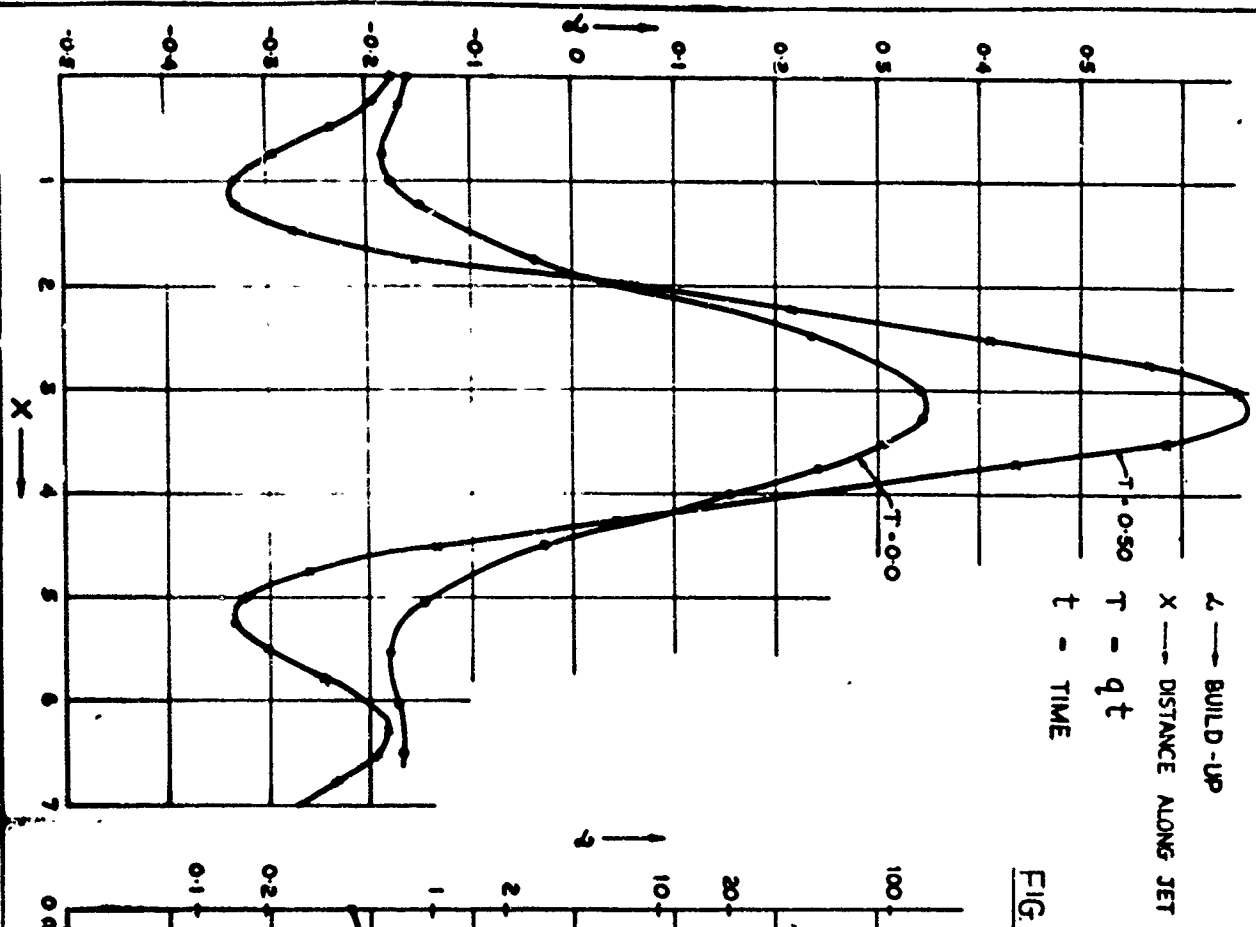
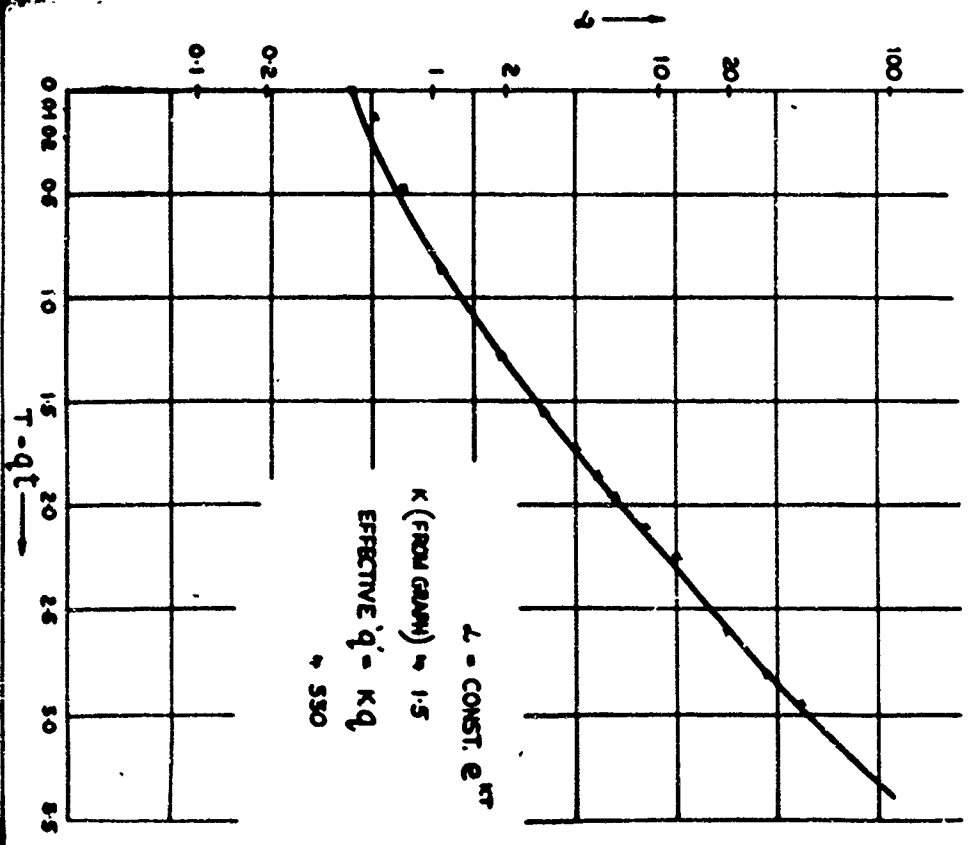


FIG. 5 BUILD-UP VERSUS EXPONENT VALUE



The series represented by equation (3.20) becomes divergent for an  $\frac{A}{qa}$  value over one. So the analysis would break down in this case for a value of velocity modulation above about 12 cm/sec. This is all right within the initially assigned limits of very small initiating modulation amplitudes. At higher amplitudes the analysis would have to be replaced, as liquid bunching as well as capillary instability must be taken into account.

It is felt that the above analysis is an improvement on the original Rayleigh analysis as

- (a) the physical nature of the initiating disturbance is identified and incorporated in the theory.
- (b) the analysis has been extended to the second order and thus can be expected to be accurate for appreciable sized corrugations on the jet.

Section 4. A Theory for Jet Break-up in the Case of Large Velocity Modulation Amplitudes.

The velocity modulation in this case not only triggers the capillary instability but causes liquid bunching along the jet (a forced radial compounded velocity is introduced).

Bunching Theory

As a preliminary step the bunching mechanism will be considered and mathematically defined. The jet can be considered as a system for particles without surface tension or interaction.

The velocity of particles emerging from the orifice at time  $t = t_0$ , is written as

$$u_1 = u_0 + u' \sin \omega t_0 \quad \text{----- (4.1)}$$

where  $t_0$  is the time original at the nozzle.

$u_0$  is the steady velocity

$u'$  is the modulation amplitude.

The time of arrival of a particle at a plane  $z$  is given by

$$t_1 = t_0 + \frac{z}{u_0(1 + \frac{u' \sin \omega t_0}{u_0})} \quad \text{----- (4.2)}$$

$$\therefore t_1 \doteq t_0 + \frac{z}{u_0} - \frac{z u'}{u_0^2} \sin \omega t_0 \quad \text{----- (4.3)}$$

As the flow is continuous, if  $n_0$  is the particle current at the orifice, then

$$n_0 dt_0 = n_1 dt_1 \quad \text{----- (4.4)}$$

$$\frac{dt_1}{dt_0} = 1 - \frac{\omega z u'}{u_0^2} \cos \omega t_0$$

$$\therefore n_1 = \frac{n_0}{1 - \left( \frac{\omega u' z}{u_0^2} \right) \cos \omega t_0} \quad \text{----- (4.5)}$$

If the particle density is constant, then

$$\frac{n_0}{n_1} = \frac{r_0^2}{r_1^2}$$

where  $r_0, r_1$ , are the radii of the jet. The following expression for the radius of the jet at any time  $t_0$  (in the orifice frame of reference) is obtained:

$$r_1 \doteq r_0 \left\{ 1 + \frac{1}{2} \cdot \frac{\omega \omega'}{\omega_0^2} \cos \omega t_0 \right\} \text{----- (4.6)}$$

It may be sometimes more useful to consider the various harmonics separately, as the above expression assumes that they are equally attenuated. So we expand out  $n_1$ , of equation (4.5) in a Fourier series in the angle  $\omega(t - \frac{z}{u_0})$ . Considering the first harmonic only, leads to the following expression for  $n$ :

$$n_1 = n_0 \left[ 1 + 2 J_1 \left( \frac{z \omega' \omega}{u_0^2} \right) \cos \omega t \right] \\ = n_0 \left[ 1 + 2 J_1 \left( \frac{z \omega' \omega}{u_0^2} \right) \cos k z \right] \text{----- (4.7)}$$

where  $z = u_0 t$ ,  $k = 2\pi/\lambda$ , and the time scale has been changed to that of the moving jet.

In Fig. 6 the build-up profile for the case of all harmonics present is shown. It would indicate that with pure bunching (non-interacting particles), discs would be formed along the jet. As will be seen later, this prediction was strikingly confirmed for the case of very high 'g' vibration. Under these conditions appreciable velocity modulation is induced and so the 'bunching' action predominates over surface tension effects. The non-interaction condition on which the above equation (4.7) is based, would then naturally be a more realistic approximation.

#### Jet Analysis

The Rayleigh procedure was followed closely, but the surface position equation was modified to include a 'bunching' term:

$$r = a_0 + \Delta \cos k z + f(z) \\ = a_0 + \Delta \cos k z + \frac{a_0}{2} \cdot \frac{\omega \omega'}{\omega_0^2} \cos \omega t \text{----- (4.8)}$$

This leads to changes in both the kinetic and potential energy terms. The kinetic energy must now include the transverse velocity component.

The expression for  $a$  now becomes,

$$a^2 = a_0^2 + \frac{1}{4} d^2 + \frac{a_0^2 \beta^2 u'^2 \omega^2}{4 u_0^4} \quad \text{-----(4.9)}$$

and so

$$a_0^2 = (a^2 - \frac{1}{4} d^2) / (1 + \frac{\beta^2 u'^2 \omega^2}{4 u_0^4}) \quad \text{-----(4.10)}$$

Note: the cosine term in the 'bunching' expression is taken as unity, so that only the profile of maxima in the build-up will be obtained.

The potential energy,  $P$ , per unit length now is given by the following relation:

$$P = \frac{\pi a T}{4} \left\{ \frac{d^2}{a} \left( \frac{1}{2} \frac{\beta^2 u'^2 \omega^2}{4 u_0^4} - 1 \right) + \frac{1}{4} k^2 d^2 + \frac{u'^2 \omega^2}{u_0^4} (1 + k^2) \cdot \frac{(a^2 - \frac{1}{4} d^2)}{(1 + \frac{\beta^2 u'^2 \omega^2}{4 u_0^4})} \right\} \quad \text{-----(4.11)}$$

#### Kinetic Energy Term

If  $\phi$  is the velocity potential then the axial and transverse velocities are given by

$$\begin{aligned} u &= -\frac{\partial \phi}{\partial z} \\ v &= -\frac{\partial \phi}{\partial r} \end{aligned} \quad \text{-----(4.12)}$$

$$\text{Now } \phi = A e^{qz} \cos\left(\frac{p z}{a}\right) J_0\left(\frac{j k r}{a}\right) \quad \text{-----(4.13)}$$

where  $p = k a = \frac{2\pi}{\lambda} a$

$K$ , the kinetic energy per unit length, is given by

$$K = \frac{1}{2} \int_{-\frac{2\pi a}{\lambda}}^{\frac{2\pi a}{\lambda}} dz \int_0^a \left[ (J_0(j k r))^2 + (J_0'(j k r))^2 \right] r dr \quad \text{-----(4.14)}$$

and using the relations (4.12) and  $p^2 = k^2 a^2$ , we get

$$K = 2\pi^2 k A^2 e^{2qz} \int_0^a \left[ (J_0(j k r))^2 + (J_0'(j k r))^2 \right] r dr \quad \text{-----(4.15)}$$

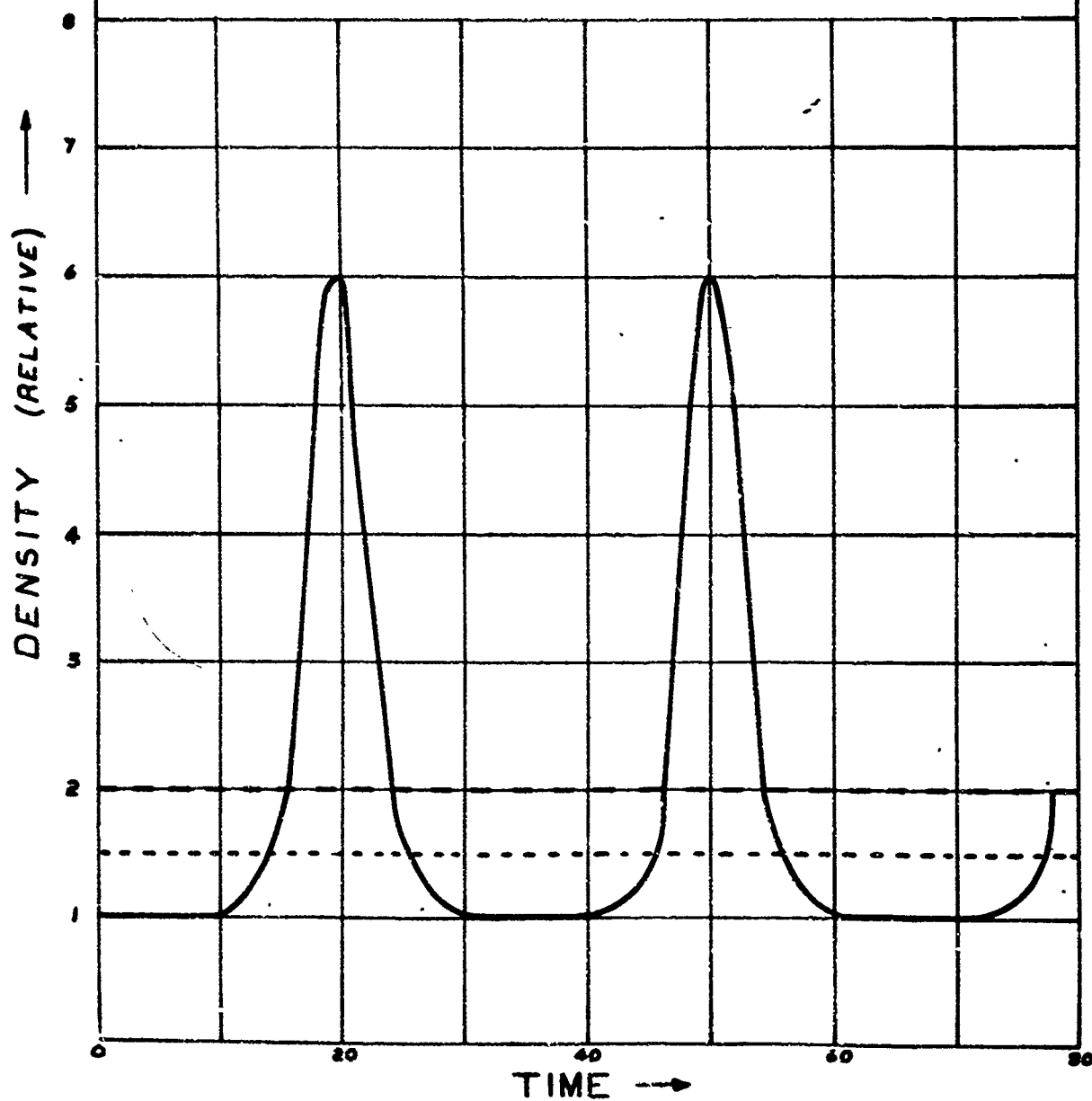
The Bessel functions are now expanded out as series, terminating these at the third and second terms, respectively.

The final expression for  $K$  is,

$$\begin{aligned} K &= \pi^2 a^2 k A^2 e^{2qz} \left[ 1 + \frac{a k^3}{4} - \frac{a k^2}{4} + \frac{3 a^3 k^4}{5 \cdot 2^4} + \dots \right] \\ &= \pi^2 a^2 k A^2 e^{2qz} [2.7] \end{aligned}$$

**Fig. 6**      **SCHEMATIC OF THE PARTICLE DENSITY**  
**PROFILE IN THE PRESENCE OF VELOCITY MODULATION**

**NOTE : THE DIAGRAM IS FOR NEARLY PURE BUNCHING**



Using the Lagrange equation for a conservative system,

$$\frac{d}{dt} \left( \frac{\partial K}{\partial \dot{z}} \right) - \frac{\partial K}{\partial z} + \frac{\partial P}{\partial z} = 0$$

and considering maxima only ( $\cos k_z = 1$ ), the following equation of motion is obtained,

$$\frac{d^2 z}{dt^2} + \frac{z}{2} \left\{ \left( J_0'(jkr) \right)^2 \frac{kT}{2\pi a} \left[ \frac{1}{a^2} \left( 1 - \frac{u^2 \omega^2 t^2}{4 u_0^2} \right) - k^2 - \frac{u^2 \omega^2}{8 u_0^4} \left( 1 - \frac{u^2 \omega^2 t^2}{4 u_0^2} \right) \right] \right\} = \frac{2 J_0''(jkr)}{J_0'(jkr)} \cdot z \quad (4.17)$$

It must be noted that in deriving this equation all the harmonics were assumed to be present and so it will be strictly only valid for the conditions of strong bunching (very high 'g' high frequency vibration). For the transition region where capillary and bunching action are roughly of the same effectiveness, an analysis based on equation (4.7) would probably be more appropriate.

#### Method of Solution

Equation (4.17) must be solved for  $z$  as a function of time. This can only be done numerically. Now  $T$  is a function of both  $z$  and  $t$  and so one is forced to compute  $z$  for a small interval of time, compute  $T$  and then use this value in the computation of  $z$  at the end of the next time interval.

The 4th order Runge-Kutta technique for integrating differential equations was found to be the most suitable for this purpose.

When  $z$  is determined for a step, the new  $T$  value is computed and this is used in equation (4.8) in computing  $z$  at the end of the following step.

This procedure appears to give satisfactory results. The programme was written in Fortran and executed on the IBM 1620 digital computer. Bessel functions were evaluated in the programme using the continued fraction approximation. This increases computing time greatly, however.

There is no theoretical analysis available for predicting the velocity modulation induced by a particular vibration frequency and  $\mu'$  value.

The range of values was chosen on the basis of the observed pressure variations in the cavity as reported in Section 2.

For a 1000 cm/sec jet,  $\mu'$  values from about 3 cm/sec to 50 cm/sec were used.

This would correspond roughly to acceleration values from about 5 to 50 'g'. Modulation values less than about 5 cm/sec would be only capable of initiating capillary type instability.

The region from 5 to 30 cm/sec is transitional, where capillary action and bunching are almost equally effective.

In the region over 30 cm/sec liquid 'bunching' becomes predominant.

The break-up length criterion has been interpreted as that point on the jet where the maxima, or  $L$ , has reached a value equal to the original jet radius. It has significance at low or intermediate modulation values, where bunching action is small. However with strong bunching, it loses its significance as a criterion. Disc formation corresponding to  $L$  values of many times the original radius is very rapid, but actual break-up is delayed till capillary action thins out the liquid cylinder joining the discs.

Thus, comparisons of experiment and theory on the basis of break-up measurements, is only possible in the low and intermediate 'bunching' regions.

In practice, moreover, small random fluctuations in pressure are always present, and so one cannot have zero velocity modulation as in theory. To make the above theory more realistic, then, a small constant modulation term  $\xi_0$ , was included in the formula, where  $\mu' = \mu_1 + \xi_0$

In the 1000 cm/sec case taken as an example,  $\epsilon_0$  was given a value of 2 cm/sec.

#### Comparison of Theoretical and Experimental Results

The above analysis was applied to the case of a water jet at 1000 cm/sec. velocity, with an applied vibration frequency of 2000 cps. The wave-length on the jet was thus 0.5 cms (near the middle of the Rayleigh spectrum).

Graphs of build-up (profile of maxima) on the jet versus time are shown in fig. 7 for 2 cases. The curve for low driving amplitudes (weak velocity modulation) indicates a fairly rapid initial build-up, then a slow increase and final rapid 'break-up'.

The experimental result, using the travelling microscope technique, is shown to resemble it in outline (of course the initial region cannot be checked as the maxima are too small to be observed).

The curve for higher velocity modulation (30 cm/sec) shows the rapid build-up which results. The break-up criterion corresponds to an ordinate value of .06, and has no significance in this case as mentioned above. Plate 11. shows the result observed for strong bunching. This was a water jet subjected to a vibration acceleration value of about 60 'g' at 3,000 cps. The rapid disc formation is characteristic of 'bunching' in which all the harmonics are present. The disc reached a certain size and final break-up occurs further down the jet and is due to capillary action on the cylinder connecting the discs. The bulge midway between the discs indicates the build-up of other harmonics.

The observation of disc formation is striking confirmation that the driving force is velocity modulation.

# THEORETICAL PREDICTION OF AMPLITUDE BUILD-UP VERSUS TIME

$U$  - JET VELOCITY - 1000 cm./sec.  
WAVELENGTH - 0.5 cms.

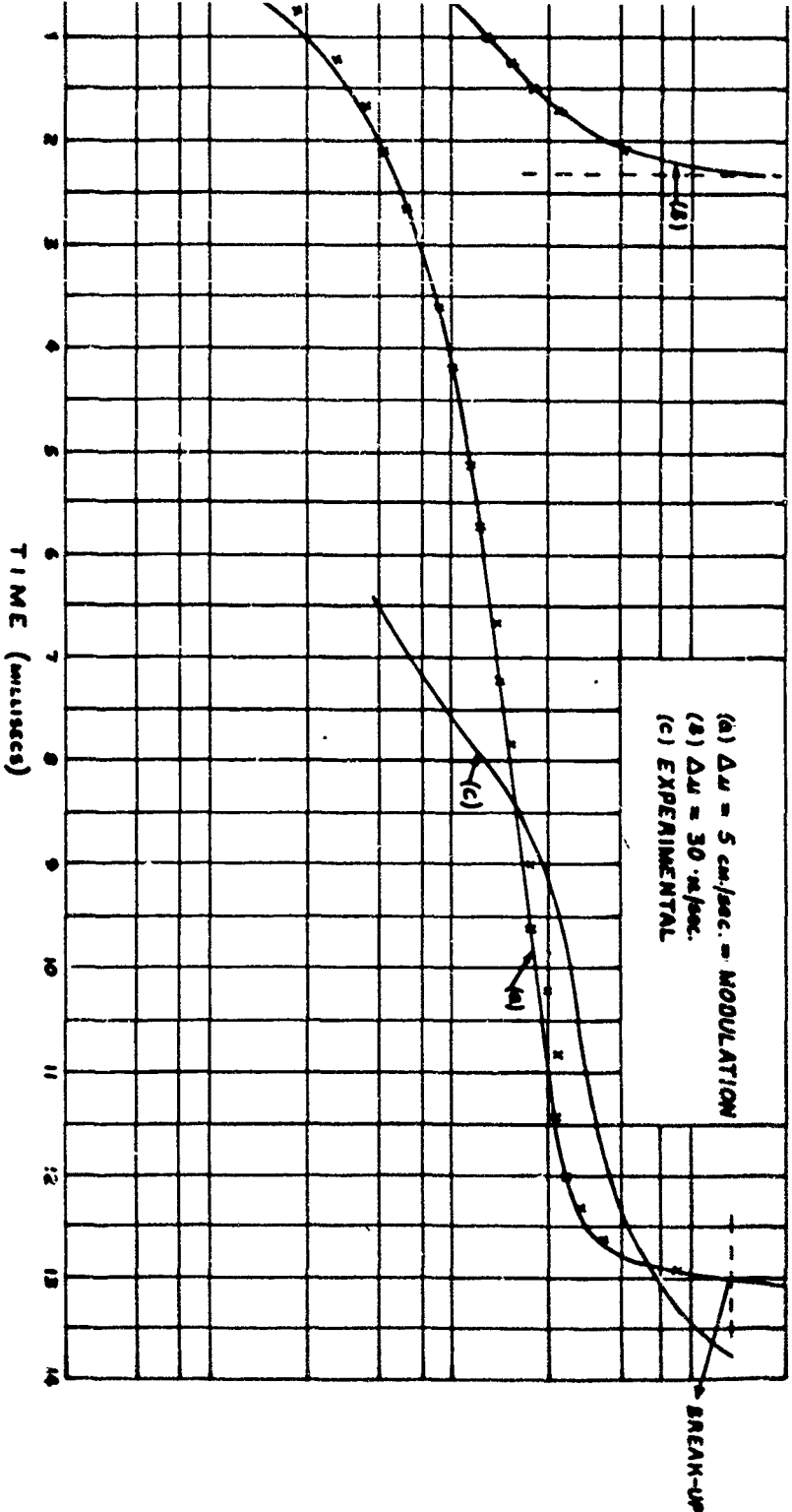


**FIG. 8**

**BREAK-UP LENGTH VS VELOCITY MODULATION - THEORETICAL -**

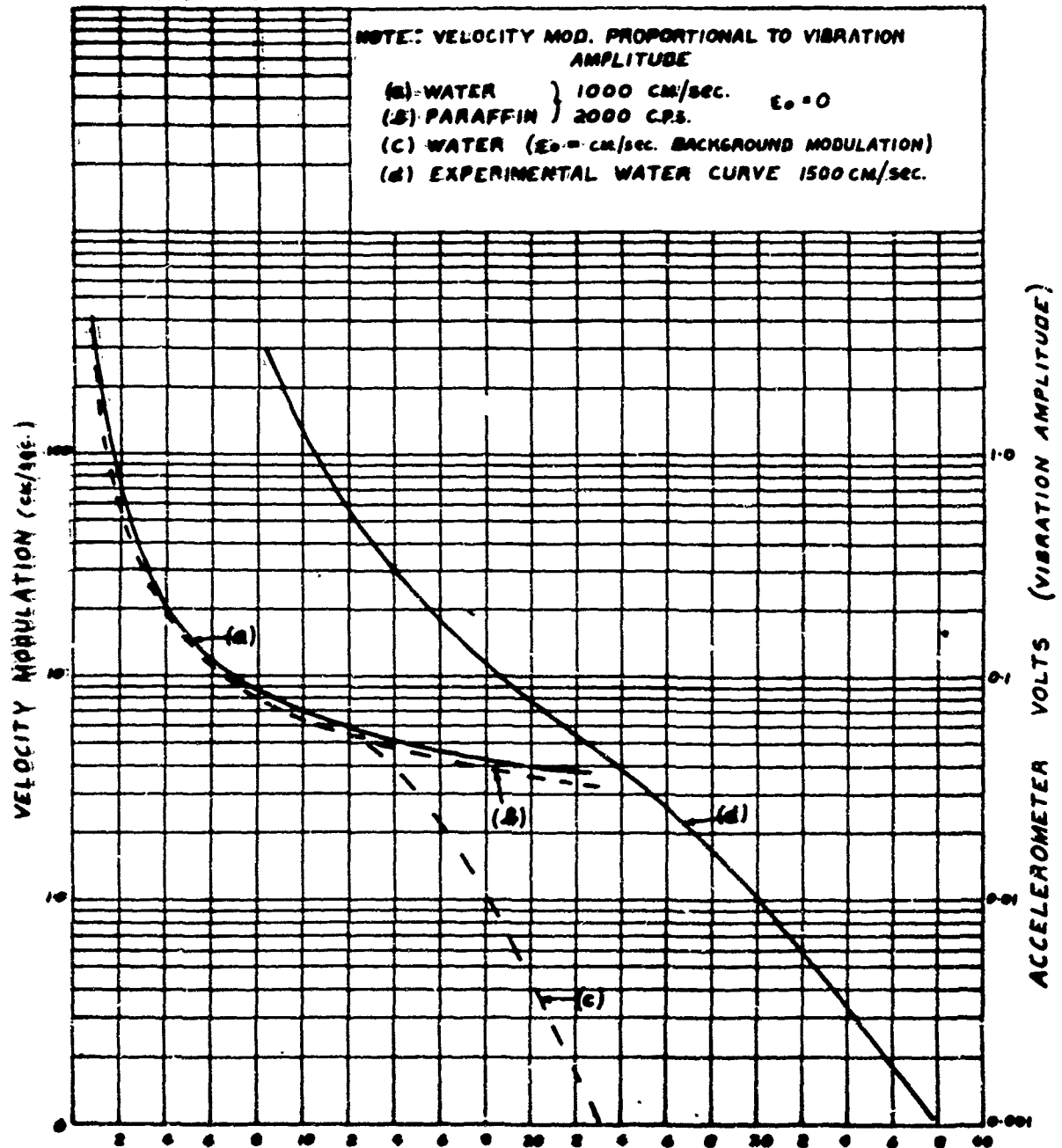


Plate III. shows a similar phenomenon for a paraffin jet.

Most of the experimental measurements made on the jet have been of actual measured break-up length versus vibration amplitude. To realistically compare theoretical results with these, break-up lengths (based on the radius criterion) for a range of  $U$  and intermediate modulation values, were computed for the 1000 cm/sec. jet. Vibration amplitude and velocity modulation are considered as proportional parameters.

Results shown in Fig. 8 curves (a) and (b) are for water and paraffin jets.

The theory predicts little difference in their behaviour in the finite modulation velocity region. Curves (c) and (d) are experimental ones for paraffin and water jets at about 1200 cm/sec.

The experimental curves also show that in the finite modulation region, the behaviour of paraffin and water is indeed similar (and presumably this will be even more so at higher modulation values).

There is enough agreement between the above analysis and experimental results to confirm that it is largely correct.

The photographs of jet break-up obtained by Reba and Brosilow and Miesse indicate that the velocity modulation obtained by them falls in the very low category, covered by the analysis in Section III. Thus, the variation of pressure downstream of the injector is not an efficient method of producing velocity modulation.

### Section V. Conclusions

It seems fairly conclusive that the rotationally symmetric disturbance required to trigger the Rayleigh-Weber capillary instability on liquid jets, may be physically attributed to velocity modulation. This would be induced by pressure variation upstream of the injector throat. Under normal circumstances, minute random pressure fluctuations will always be present in the cavity behind the injector.

The application of mechanical vibration in the appropriate frequency range and at small vibration acceleration values can induce such minute pressure fluctuations and trigger the capillary instability. The theory expounded in Section 3 is considered to cover this case.

With high vibration acceleration, finite velocity modulation values can be produced. This produces an appreciable 'bunching' effect in the liquid jet, and if strong enough it will predominate over the capillary effect. The analysis in Section 4 is given as a semi-quantitative theory of the phenomenon as observed in the transition region between the predominant capillary region (infinitely small 'bunching') and the predominant 'bunching' region.

However, a criterion to replace the break-up length  $l_b$  (used with success in the very low 'bunching' region) is necessary to allow satisfactory comparison between theory and experiment.

The analysis predicts that under strong 'bunching' conditions (induced by high frequency, high 'g' vibration), the behaviour of various liquids will be very similar. Experiment confirms this. Some variations will be expected due to the variation in elastic properties of liquids. For a given vibration, more or less velocity modulation may be produced depending on the

relaxation constants of the liquid. However as the analysis took velocity modulation as a basis, this did not apply to the theory, but would have affected the experimental results somewhat.

In the region of predominant bunching and disc formation, the restriction to low velocity laminar jets is not necessary. The results for water at 95 and 145 fps are shown in Plates IV and V. (taken under 200g's of vibration at 4,500 cps).  
1,800

Spreading of the liquid is caused by aerodynamic fragmentation, but the definite mass concentration spaced at wave-length distances along the jet, is still very evident.

It is of interest to note that single discs have been observed previously on liquid jets.<sup>(9)</sup> They were induced by the application of a step change in velocity at the orifice. The analysis given was rather crude and would not cover the low modulation velocity region. However the evidence for velocity modulation at the orifice being the cause of the phenomena reported here, must now be regarded as complete.

Prediction of the magnitude (and phase) of velocity modulation produced by a given vibration is a necessary next step. From the vibration point of view it will render the analysis more complete. Further investigation of the effect of vibration on the injector cavity hydrodynamics is planned.

References

1. "Investigation of the Effect of Mechanical Vibration on the Break-up of a Liquid Jet in Air" McCormack, P.J., Birch, S., Crana, L.  
British Journal of Applied Physics (Vol.15 June, 1964, Pages 743-750).
2. "On the Instability of Jets" Rayleigh, Lord, Proc. of the London Math. Soc. Vol. 10 (1878) p.4.
3. "On the Break-down of a Fluid Jet" Weber, C., ZAMM Vol.11 (1931) p.136.
4. "Effect of Ambient Pressure Oscillation on the Disintegration and Dispersion of a Liquid Jet" Miesse, C.C., Journal of the American Rocket Society, Vol. 25 No.10 (1955).
5. "The effect of Sound on Liquid Jets" Castineau, B.G.  
Aero Jet-General Company Progress Report No.4, February, 1954
6. "The Response of Liquid Jets to Large Amplitude Sonic Oscillations" Rehn, L., & Brosilow, C., WADC Technical Report 59-720 Part 111 September (1960).
7. "The Laminar Boundary Layer on Oscillation Plates and Cylinders" Glauret, E., J. Fluid Mechanics 1 97-110 (1956)
8. "Berechnung ebener Periodischer Grenzschichtströmungen" Schlichting, H., Phys. J. 33 327 (1933)
9. "Velocity Discontinuity Instability of Liquid Jet" Dunne, J., and Casson, B. Journal of Applied Physics Vol. 27 No.6. June (1956) p. 577.

Part 3 (a)

PROPERTIES OF TAYLOR VORTICES OF LARGE AMPLITUDE

This paper is concerned with the secondary vortex flow of fluid between two concentric cylinders; the inner cylinder rotates at a constant speed while the outer is kept fixed. Taylor (1923) has shown that as the speed of the inner cylinder is increased beyond a certain value the motion changes from a purely tangential flow to one in which there exists a superposed secondary vortex flow. The vortices in this flow are in the shape of toroids whose axis is the axis of the cylinders. Taylor predicted the conditions under which this transition takes place; he also gave the form of the infinitesimal vortices. The extension to rates of rotation above the critical value, when the amplitude of the secondary flow is an appreciable fraction on the main flow, was made by Stuart (1958).

Taylor confirmed experimentally his theoretical value for the critical speed; his value has also been verified by the experiments of Wendt (1933) and Donnelly and Simon (1960) who also confirmed Stuart's analysis. Donnelly and Simon show, however, that Stuart's analysis holds only for a limited range of speeds above the critical. It is the aim of this paper to give an approximate analysis of the flow when the rates of rotation are so large that Stuart's analysis is no longer valid.

The reason for the occurrence of these vortices lies in the centrifugal force field set up by the primary flow. When the motion is purely tangential, the speed of the fluid decreases linearly outwards from the peripheral speed of

the inner cylinder to rest on the outer cylinder. There exists, therefore, a tendency for a fluid particle to migrate from the inner cylinder to the outer. This tendency will be realised when the centrifugal force is sufficient to overcome the viscous forces in the fluid. The ratio of these forces is given essentially by the non-dimensional Taylor number  $T$ , defined by

$$T = \frac{h}{R} \left( \frac{U h}{\nu} \right)^2$$

where  $R$  is the radius of the inner cylinder,  $h$  is the gap between the cylinders and  $U$  is the peripheral speed of the inner cylinder, and  $\nu$  is the kinematic viscosity.

Taylor showed that vortices were set up when the Taylor number was greater than about 1700. When  $T$  is greater than 1700 a range of vortex shapes will be amplified; the form which has the greatest amplification has an approximately square cross-section, this form ultimately predominates.

In this paper it is shown by an approximate method that the drag on the inner cylinder is increased by these vortices in the ratio

$$0.3 T^{1/4}$$

when  $T > 10^4$ . This result agrees well with the experimental results of Taylor and Wendt quoted above, provided the Reynolds number  $U h / \nu$  is less than about 5,000, above which value the flow becomes turbulent.

#### References

- Donnelly, R.J. and Simon W.J. (1960) J. Fluid Mech. 7, 401  
Stuart, J.T. (1958) J. Fluid Mech. 4, 1.  
Taylor, G.I. (1923) Phil. Trans. A.223, 289.  
Wendt, F. (1933) Ingen. -Arch. 4, 577.

Part 3 (b)

TITLE:

"The Tangential Mode and Rocket Engine Burn-Out"

Authors: DR. L.J. CRANE  
MR. S. BIRCH  
DR. P.D. McCORMACK.

Nomenclature:

- $U_{\infty}$  = free stream velocity
- $u_0(y)$  = x - component of velocity in the boundary layer  
in the absence of vortices
- $(u_1, v_1, w_1)$  = the additional velocity components due to the  
disturbance
- $(u_L, u_R)$  = the x - components of velocity at the edges of  
the regions of abrupt change
- $\omega$  = vorticity in the x - direction
- $\delta$  = thickness of the boundary layer
- $\gamma$  = kinematic viscosity
- $Re = U_{\infty} \delta / \gamma$  = Reynolds Number
- $\varepsilon$  = thickness of the region of abrupt change in the cell.
- $\psi$  = pseudo stream function
- $R$  = radius of curvature of the wall
- $F$  = skin friction ratio
- $\beta$  = amplification factor for small amplitude values
- $\lambda$  = wave-length in the z-direction
- $\alpha$  =

### INTRODUCTION

It is contended here that the impingement of rotating gas on the wall of a cylindrical rocket engine chamber, as will occur in the presence of tangential (although this involves an oscillating flow) and spinning modes of instability, will result in the three-dimensional type of boundary layer instability first designated by Taylor<sup>(1) (2)</sup> for the case of rotating concentric cylinders and later by Görtler<sup>(3)</sup> for gas flow over a concave surface.

The formation of the regular and well-ordered pattern of Taylor-Görtler vortices, with axes parallel to the chamber wall, will be shown to result in a very large, albeit oscillating, increase in heat flux to the wall over that due to normal convection.

The coordinate system used by Görtler (see "Boundary Layer Theory" by H. Schlichting p.442) will be adopted in this work,

x = coordinate in the cylinder wall and parallel to the main gas flow.

y = coordinate perpendicular to the wall

z = coordinate perpendicular to the x direction.

Görtler analysed the time build-up of the vortices by considering a small three dimensional disturbance superposed on the flow:

$$\begin{aligned}u' &= \bar{u}_1(y) \cos(\alpha z) e^{\beta x} \\v' &= \bar{v}_1(y) \cos(\alpha z) e^{\beta x} \\w' &= \bar{w}_1(y) \sin(\alpha z) e^{\beta x}\end{aligned}$$

Instability, or vortex formation, will be initiated when, for a given wave number  $\alpha$ , the characteristic parameter or Görtler Number, is above a certain critical value:

$$\frac{U_\infty \delta}{\nu} \cdot \sqrt{\delta / R} > 16$$

### Typical Engine

We have taken the experimental results quoted by H.C. Krieg Jnr.<sup>(4)</sup> for a 15 inch diameter engine, as a basis for numerical results.

Using Schlichting's formula<sup>(5)</sup> for the boundary layer on a smooth plate, and taking a free stream velocity of 2000 fps and a maximum available time of  $10^{-2}$  sec, a mean boundary layer thickness,  $\delta$ , of about  $3.5 \times 10^{-3}$  ft. is obtained.

For Krieg's chamber,  $R = 7.5$  inches and so

$$\text{Görtler Number} = \frac{U_{\infty} \delta}{\nu} \cdot \sqrt{\delta/R} = 460.$$

The condition for instability is thus satisfied.

An arbitrary initial disturbance will have a range of Fourier components which will be amplified. The component with the greatest amplification factor corresponds to a cell structure whose wave-length is about  $2\delta^{(3)}$ . This cell size will ultimately predominate.

In the case considered above,  $\beta$  for this type of cell is about 40,000. Thus, the initial rate of build-up is about  $e^{40,000t}$ . Kirchgassner<sup>(6)</sup> has proved that a finite upper bound for the vortex growth exists, this being when the vortex velocity equals the free stream rotational velocity. It is thus certain that the vortices will have reached their maximum size in a time well under  $10^{-2}$  sec. The ultimate (steady-state) vortex structure will have a wave-length of about  $2\delta$ .

### Analysis

The equations of motion as developed by Görtler, and neglecting terms containing  $\delta/R$ , are as follows:

$$\frac{\partial \psi}{\partial z} \left( \frac{\partial u_0}{\partial y} + \frac{\partial u_1}{\partial y} \right) - \frac{\partial \psi}{\partial y} \cdot \frac{\partial u_1}{\partial z} = \nu \nabla^2 u_1$$

----- (1)

$$\frac{\partial \psi}{\partial z} \cdot \frac{\partial u_1}{\partial y} - \frac{\partial \psi}{\partial y} \cdot \frac{\partial u_1}{\partial z} + \frac{2}{R} \frac{\partial u_1}{\partial z} (\mu_1 + \mu_0) = \nu \nabla^2 \omega \quad (2)$$

$$\omega = \nabla^2 \psi \quad \text{--- (3)}$$

where  $\psi$  is a pseudo stream function, defined by

$$v_1 = \frac{\partial \psi}{\partial z}, \quad u_1 = \frac{\partial \psi}{\partial y} \quad \text{---- (4)}$$

and  $\omega$  is the component of vorticity in the x direction,

$$\omega = \frac{\partial v_1}{\partial z} - \frac{\partial u_1}{\partial y} \quad \text{---- (5)}$$

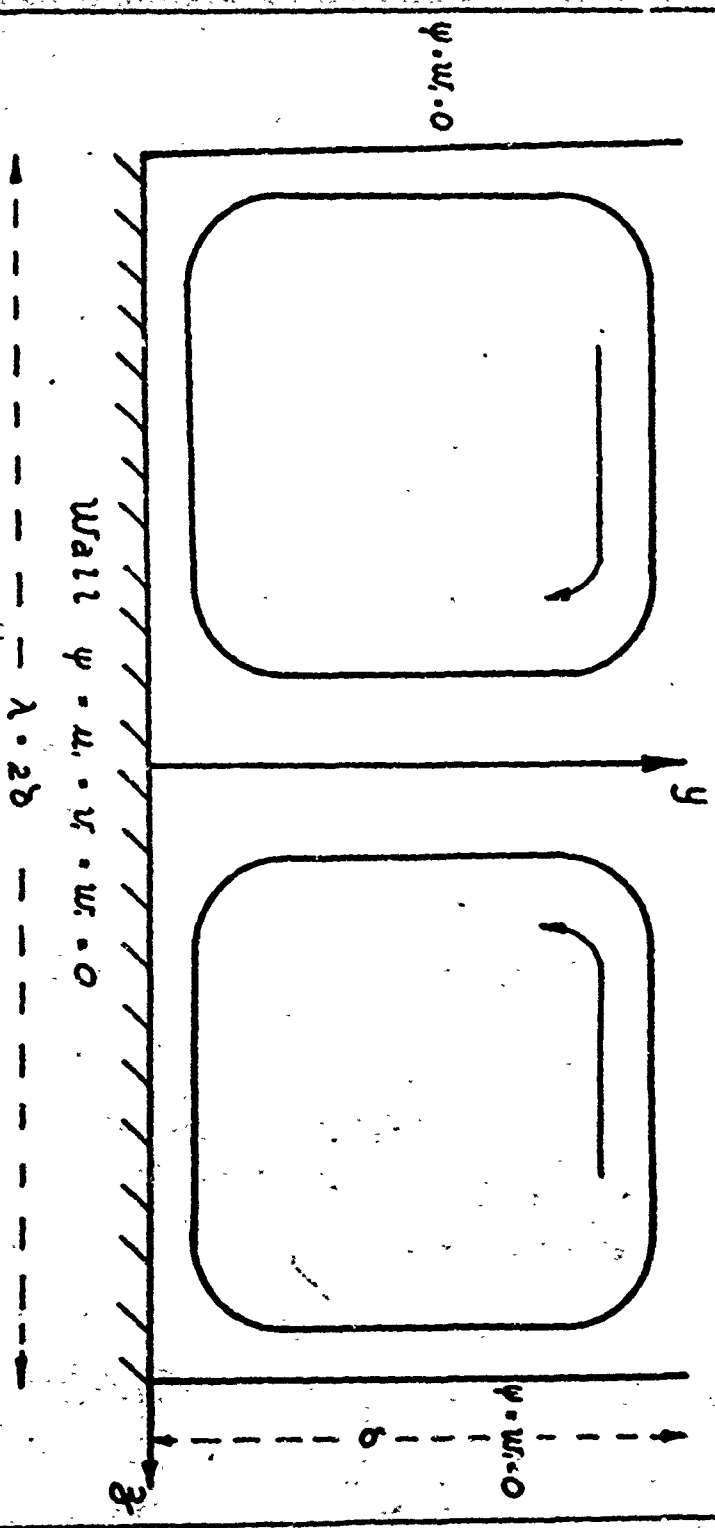
The boundary conditions over a single cell (one wave-length, two vortices) are as shown in Figure 1.

Note: all the quantities are periodic in the z direction.

This means in particular that  $\mu_1, v_1, \omega$  have the same values at the outside edges of the cell respectively.

FIG. 1

Free-Stream :  $u = U_{\infty}$  ;  $\psi = u \cdot v = w = 0$



By an order of magnitude procedure it will be shown that the rate of change of the various parameters,  $\omega$  etc., cannot be of the order  $\omega/\delta$  etc., over all the cell.

Suppose the variation is  $\frac{\omega}{\delta}$  etc.

Consider equation (2): Term by term this leads to Table I

Table I

$\frac{\partial \psi}{\partial z} \frac{\partial \omega}{\partial y} - \frac{\partial \psi}{\partial y} \frac{\partial \omega}{\partial z}$	$\frac{2}{R} \frac{\partial}{\partial z} (\mu_0 + \mu_1)$	$\gamma \nabla^2 \omega$
$v_1 \frac{\omega}{\delta}$	$\frac{1}{R} \cdot \frac{\mu_1}{\delta} \cdot \mu_0$	$\gamma \frac{\omega}{\delta^2}$
$\frac{R}{\delta} \cdot \frac{v_1^2}{\mu_0 \mu_1}$	1	$\frac{v_1 \cdot R}{\mu_1 \cdot \delta}$

Note:  $\omega \div v_1/\delta$

Consider equation (1): Term by term this leads to Table II.

Table II

$\frac{\partial \psi}{\partial z} \left( \frac{\partial \mu_0}{\partial y} + \frac{\partial \mu_1}{\partial y} \right) - \frac{\partial \psi}{\partial y} \frac{\partial \mu_1}{\partial z}$	$\gamma \nabla^2 \mu_1$
$v_1 \cdot \frac{\mu_0}{\delta}$	$\gamma \cdot \frac{\mu_1}{\delta^2}$

Hence  $v_1 = \frac{\mu_1}{Re}$ , where  $Re = U_\infty \delta / \nu$

Putting this value for  $v_1$ , into the expressions in Table I, the bottom row now becomes, as shown in Table III.

Table III

$\frac{\mu_1}{\mu_0} \cdot \frac{R}{\delta} \cdot \frac{1}{Re^2}$	1	$\frac{R}{\delta} \cdot \frac{1}{Re^2}$
---	---	---

The first and third terms are vanishingly small ( $10^{-5}$ ), implying that the boundary conditions cannot be satisfied. We must infer then, that  $\omega$ ,  $\mu$ , etc. only change slowly over most of the cell, there being a thin region where very abrupt parameter changes occur. Let its width be designated by the symbol  $\xi$ . The cell (see Fig. 2) now consists of two regions, 'slow' and 'abrupt' respectively.

In the slow region the viscous terms in the equations can be neglected. Now  $\mu_0 = \mu_0(y)$ , and so equation (1) can be written as,

$$\frac{\partial \psi}{\partial z} \cdot \frac{\partial \mu}{\partial y} - \frac{\partial \psi}{\partial y} \cdot \frac{\partial \mu}{\partial z} = 0 \text{ or Jacobian } \left( \frac{\psi, \mu}{y, z} \right) = 0.$$

where  $\mu = \mu_0 + \mu_1$ . This implies that  $\mu = \mu(\psi)$  so that in the 'slow' region,  $(\mu_0 + \mu_1)$  is a constant along a stream-line.

Derivation of  $\xi$  in terms of  $\delta$ :

In the 'abrupt' region we have from equation (1),

$$v_1 \cdot \frac{\mu_0}{\delta} = \frac{\gamma \mu_1}{\xi^2}$$

Note: the variation of parameters as  $1/\delta$  or  $1/\xi$  can be assumed here.

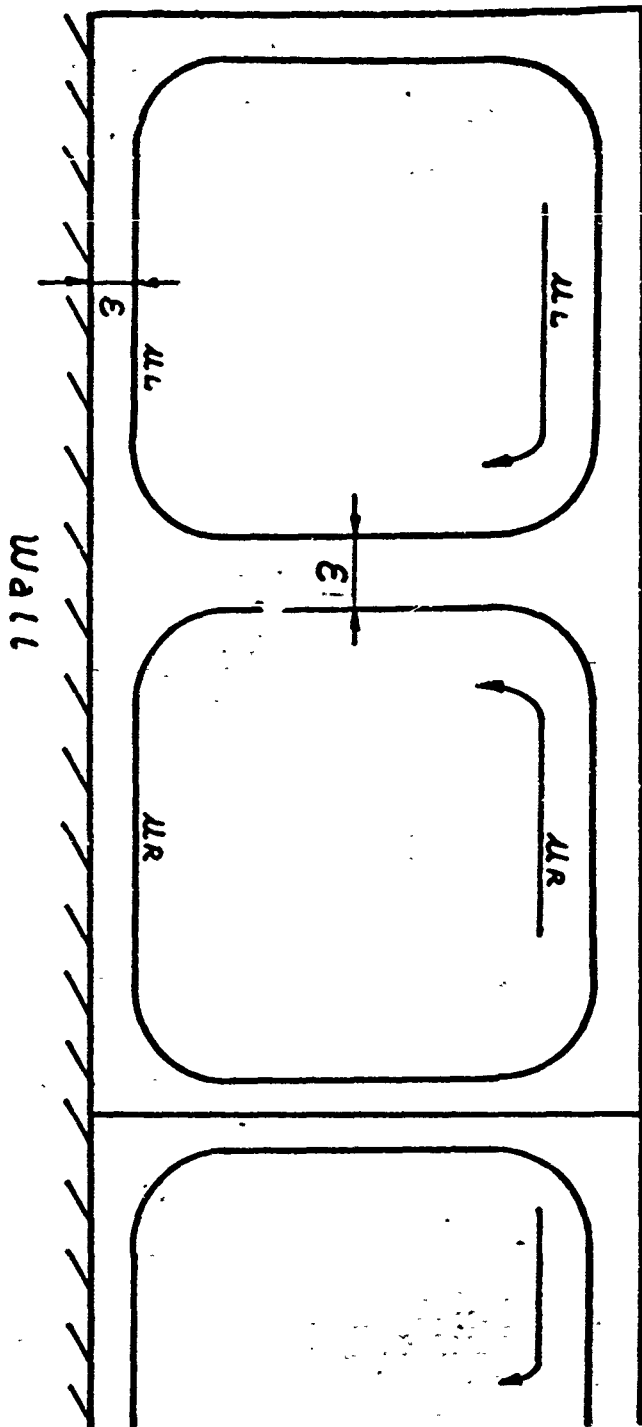
Now 
$$\omega \doteq \frac{v_1}{\xi}$$

and so

$$\omega = \frac{1}{Re} \cdot \frac{\mu_1 \delta^2}{\xi^3}$$

Fig 2

$$\mu = U_{\infty}$$



In equation (2), taking the last term on the left hand side as the dominant one,

$$\frac{1}{R} \cdot \frac{\mu_1}{\varepsilon} \cdot \mu_0 \doteq \frac{\gamma \omega}{\varepsilon^2}$$

$$\therefore \omega \doteq Re \cdot \frac{\varepsilon}{R \delta} \cdot \mu_1 \quad \text{--- (7)}$$

Combining equations (6) and (7),

$$\left(\frac{\varepsilon}{\delta}\right)^4 \doteq \left(\frac{1}{Re^2} \cdot \frac{R}{\delta}\right) \quad \text{--- (8)}$$

In the case considered here, it is found that  $\varepsilon/\delta \doteq \frac{1}{20}$

That is, the 'abrupt' region width is about 1/20 of the boundary layer width.

#### Estimation of the Heat Transfer Effect

It was decided to arrive at an estimate for this effect by defining a factor

$$F = \frac{\text{skin friction due to}}{\text{skin friction without}} = \frac{\text{heat transfer with vorticity}}{\text{heat transfer without vorticity}}$$

The cell structure arrived at is sketched in Fig.2.

Since it has been proved that  $\mu$  along a streamline in the inviscid region is a constant, let  $\mu$  have the constant values  $\mu_L$ ,  $\mu_R$  in the streamlines just outside the region of abrupt change, in the two halves of the cell respectively.

The x-component of momentum transferred from the main stream to the cell must be equal to the skin friction at the wall. Hence,

$$\gamma \left[ \left( \frac{\mu_L - U_\infty}{\varepsilon} \right) \delta + \left( \frac{\mu_R - U_\infty}{\varepsilon} \right) \delta \right] + \gamma \left( \frac{\mu_L}{\varepsilon} \right) \delta + \gamma \left( \frac{\mu_R}{\varepsilon} \right) \delta \doteq 0$$

$$\therefore \mu_L + \mu_R \doteq U_\infty$$

As  $\mu_o(y) \doteq 0$  near the wall,  $\mu$ , has the values  $\mu_L, \mu_R$  respectively, near the wall.

Then,

$$F \doteq \left( \frac{\mu_L + \mu_R}{\varepsilon} \right) \delta / \frac{2\mu_o \delta}{\varepsilon} = \frac{1}{2} \left( \frac{\delta}{\varepsilon} \right)$$

$$\therefore F \doteq \frac{1}{2} \left( Re^2 \frac{\delta}{R} \right)^{1/4}$$

----- (9)

In the example taken here, we find that equation 9 leads to a value of F of about 10. That is, a 10 fold increase in heat flux to the wall is predicted.

#### Comparison with Published Experimental Results:

The only extensive set of data for heat transfer thro' a fluid between concentric rotating cylinders available, is that of Bjorklund and Kays <sup>(7)</sup>. This data has been correlated by Nissan & Haas <sup>(8)</sup>.

Our example, with a critical  $P$  parameter value of 12 (as per Nissan and Haas), gives a  $P/P_c$  of about 200, and thus

$$\frac{\text{Nusselt}}{(\text{Nusselt})_{\text{cond}}} = 11$$

Similarly, from the work of Donnelly, Simpson & Batchelor (9) on transfer of momentum between concentric rotating cylinders separated by a low viscosity fluid, the fractional increase in momentum transferred (due to Taylor-Görtler vortex formation) is predicted to be of the order of 20.

We understand that observations on heat transfer to the rocket engine wall in the presence of tangential instability indicate a fractional increase in the region of ten.

We may conclude therefore, that experimental evidence supports the contention that the tangential mode of instability in a rocket engine can initiate this type of disturbance in the boundary layer on the wall, and lead to an independent and significant increase in heat transfer.

REFERENCES:

- (1) Taylor, G.J.: Stability of a Viscous Liquid contained between two Rotating Cylinders. Phil. Trans. Roy. Soc. London, Series A, Vol. 223 (1923), 289-343.
  - (2) Taylor, G.J.: Stability of a Viscous Liquid contained between two Rotating Cylinders. Proc. Roy. Soc. London A, 157, 546 or 565.
  - (3) Görtler, H.: On a Three Dimensional Instability in a Laminar Boundary Layer on a Concave Surface. Nachr. Wiss. Ges. Göttingen, Math. Phys. Klasse, New Series 2 No. 1 (1940).
  - (4) Penner, S.S., and Williams, F.A., Detonation and Two-Phase Flow. Academic Press, New York (1962). pp. 339-353.
  - (5) Schlichting, H.: Boundary Layer Theory. Pergamon Press Ltd., (1955), p. 25.
  - (6) Kirchgassner, K.: The Instability of Flow between Two Rotating Cylinders in relation to Taylor Vortices. Zeits. für Ang. Math. und Physik, Vol. 12 (1961) pp. 14-29.
  - (7) Bjorklund, G.S. and Kays, W.M.: Heat Transfer Between Concentric Rotating Cylinders. Journal of Heat Transfer, August (1959), pp. 175-186.
  - (8) Nissan, A.A., and Haas, F.C.: The Hydrodynamics of Flow between Horizontal Concentric Cylinders. Chem. Eng. Soc. Vol. 11 (1959) p. 207.
  - (9) Donnelly, R.G., Simon, N.G. and Batchelor, G.K.: An Empirical Torque Relation for Super-critical Flow between Rotating Cylinders. Journal of Fluid Mechanics 7, (1960) pp. 401-18.
- Acknowledgement: This work was supported by a grant from the Office of Aerospace Research, U.S.A.F.

Part 4.

Future Work

An experimental study of a gaseous diffusion flame will be carried out in which the fuel and oxidant will be injected coaxially and the injector plate is vibrated transversely. Schlieren and spectrometric techniques will be used, and luminosity and pressure measurements made in the combustion chamber, to study the flame effects induced by fuel flow modulation. The use of gas jets rather than liquid, eliminates complications due to liquid jet break-up and evaporation.

A theoretical analysis of the flowing/reacting system in the burner will also be carried out, in which the gas flow is modulating with finite amplitude and at the applied vibration frequency. The initial analysis of a cold jet with flow modulation, injected into still air, has almost been completed. The next step will be to consider coaxial jets and then to include reaction and the chemical kinetics.